CALCULATED ENERGY LEVELS OF MUONIC ATOMS

by

KAM CHUEN KONG

B.Sc., The Chinese University of Hong Kong, 1968.

A THESIS SUBMITTED IN PARTIAL FULFILLMENT

OF THE REQUIREMENTS FOR THE DEGREE OF

MASTER OF SCIENCE

in the Department

of

Physics

Accepted for the Faculty
of Graduate Studies

[redacted]

Dean for Chm

22 October, 1971

We accept this thesis as conforming

to the required standard

[redacted] .....

.....

.....

.....

.....

September, 1971.

Supervisor: Dr. G.R. Mason

ABSTRACT

Following the method of Acker et al,[28] the binding energies of the six lowest levels of muonic atoms and the transitions among these levels are calculated by solving the Dirac equations numerically. The muon is assumed to move in a field produced by a spherically symmetric charged nucleus. The Fermi-type charge distribution with parameters c and t determined by electron scattering experiments is used in the calculation. The vacuum polarization corrections are included in the final results. It is found that the results obtained are in satisfactory agreement with the experimental data, considering that a number of theoretical corrections, even though small, have been omitted.

The calculated energies of the transitions $(2p_{1/2} - 1s)$, $(3d_{5/2} - 2p_{3/2})$, $(2s - 2p_{1/2})$ and their corresponding experimental values are used to extract the parameters c and t in the charge distribution of the lead nucleus. The functional dependence of a transition energy on the nuclear parameters is represented by an iso-energetic line on the c-t diagram.

The intersection of two iso-energetic lines determines the values of c and t . It is found that the intersection obtained when the transitions $(2p_{1/2} - 1s)$ and $(3d_{5/2} - 2p_{3/2})$ are used is in fairly good agreement with the intersection obtained when the transitions $(2p_{1/2} - 1s)$ and $(2s - 2p_{1/2})$ are used, indicating the consistency of the model used in the analysis.

[redacted]

ACKNOWLEDGEMENTS

I wish to express my thanks to Dr. G.R. Mason, my supervisor, for his advice and guidance during the course of this work. I would also like to thank Dr. R.M. Pearce and Dr. D.W. Hone for their comments and suggestions on the thesis.

This work has been supported in part by the National Research Council of Canada.

TABLE OF CONTENTS

LIST OF TABLES

LIST OF FIGURES

CHAPTER 1. INTRODUCTION

The muon is an elementary particle which was discovered in 1937 in cloud-chamber studies of cosmic rays by Neddermeyer and Anderson[1] and independently by Street and Stevenson.[2] From the results of many experiments and their interpretations, the properties of the muon are well established. It is now known that the muon is a Dirac particle which, like the electron, has spin 1/2 and has no significant interaction with nucleons aside from the Coulomb interaction. It is also known that the muon is 206.8 times heavier than the electron and has exactly the same amount of charge as the electron. The charge on the muon can either be positive (μ^+) or negative (μ^-). It is an unstable particle and decays with a half life of 2.2×10^{-6} sec. into an electron ($e^{\pm}$), a neutrino (ν_e) and an anti-neutrino ($\bar{\nu}_\mu$)

$$\mu^{\pm} \rightarrow e^{\pm} + \nu_e + \bar{\nu}_\mu \quad . \tag{1.1}$$

When muons are slowed down in a target material and captured by atoms, muonic atoms are formed. A muonic atom is a system which consists essentially of a single negative muon bound to a single atomic nucleus. Due to the fact that the muon can be considered as a heavy electron,

the muonic atom is quite similar to the electronic atom. However, because of the much larger mass of the muon, the muonic orbits are about 207 times smaller than their corresponding electronic orbits and the muonic energy levels are about 207 times greater than their corresponding electronic energy levels. The existence of the muonic atom was predicted by Fermi and Teller[4] on the basis of their calculations, and was confirmed by Fitch and Rainwater[13] in their first experiment on muonic x-rays.

In the laboratory, muonic atoms are formed according to the following steps:

1) Fast pions are first produced by bombarding a target with a high energy proton beam in an accelerator and then negative muons are produced in the decay of negative pions in flight:

$$\pi^- \rightarrow \mu^- + \bar{\nu} \quad . \tag{1.2}$$

The muons are then transported to the experimental area by means of a muon-channel which consists of bending magnets and quadrupoles. In the experimental area, muons are slowed down by degrading material and are stopped within a suitable target.

2) Inside the target, the muon loses its energy by normal ionization from high energy to, say, 2 KeV . Fermi and Teller predicted[4] the time required for this step is about 10^{-9} to 10^{-10} sec. if the target is made up of

condensed matter.

3) The muon is further slowed down from 2 KeV to thermal energy by collision with electrons of comparable velocities and then captured by an atom into high orbital angular momentum orbit to form a muonic atom. It was predicted by Fermi and Teller that the time needed for this step is about 10^{-13} sec. if the target is a metal or an insulator, and is about 10^{-9} sec. if the target is gas.

4) The muon is thought to be captured in the vicinity of the K-shell electrons; this corresponds to a muonic orbit with principal quantum number

$$n_\mu \simeq \left(\frac{m_\mu}{m_e} \right)^{\frac{1}{2}} \simeq 14 \qquad (1.3)$$

where m_μ and m_e are masses of the muon and the electron respectively. Since all muonic states are unoccupied, the muon will cascade down from this $n = 14$ orbit into lower orbits, first by Auger transition (accompanied by the emission of Auger electrons) and then by radiative transitions. Eisenberg and Kessler[5] pointed out that most of these transitions take place within a time of order 10^{-13} sec. When the muon reaches the ground state, it will either decay or will be captured by the nucleus with a half life of[6]

$$\frac{328}{Z} \times 10^{-7} \text{ sec.} \qquad (1.4)$$

where z is the atomic number of the nucleus.

The usefulness of the muon as a nuclear probe was first recognized by Wheeler,[7,8] whose original papers still serve as a basic guide to the subject. Wheeler pointed out that from measurements of muonic x-rays the shape as well as the radial extent of the nuclear charge distribution could be determined. This method for determining nuclear charge radii has been used extensively following the pioneer experiments of Fitch and Rainwater[13]. It complements the determination of the same quantity from high energy electron scattering experiments[9].

Since 1962, many careful experimental measurements of the transition energies in muonic atoms have been reported. In order to compare these experimental results with the theory and to extract information about the nuclear charge distribution from them, energy levels and transition energies of muonic atoms must be calculated. Several authors[10-12] have carried out this kind of calculation for some nuclei. In particular, Ford and Wills[10] have calculated the 2p - 1s transition energies for a large number of elements in the periodic table. In their numerical solution of the Dirac equations, they used a charge distribution which had been used previously to fit electron scattering data[14,15]. In their final results, corrections for first order vacuum polarization were included.

It was pointed out[25,29] that when the calculated energies of Ford and Wills are compared with the experimental measurements, there appeared to be a small but fairly systematic discrepancy; the observed energies were one or two percent larger than the predicted ones. It was suggested[25,29] that the discrepancy is resolved if a slightly denser charge distribution of smaller radius were used in the calculations. Pustovalov[11] has shown that better agreements with the experimental energies were obtained if the Fermi-type charge distribution was employed in the calculations.

In this thesis, the energy of the six lowest levels (1s, 2s, $2p_{1/2}$, $2p_{3/2}$, $3d_{3/2}$ and $3d_{5/2}$) and some transitions among these levels in muonic atoms are calculated. The calculations are done for most of the nuclei in the periodic table. For each of the nuclei considered, a spherically symmetric two-parameter Fermi-type charge distribution is used. This charge distribution, characterized by the half density radius c and the skin thickness t, is given by:

$$\rho(r) = \rho_o\{1 + \exp[4.4(\frac{r-c}{t})]\}^{-1} \qquad (1.6)$$

where ρ_o is the central charge density. For the calculations, the averaged value of the parameters c and t which have been used previously to fit the electron scattering data are used. (See Sections 2.2 and 4.1).

In Chapter 2, the theory of the muonic atom is reviewed and the Dirac equations for the muon in the field of a spherically symmetric charged nucleus are derived in dimensionless form.

Several radiative corrections are discussed in Chapter 3. Among all the possible corrections, the vacuum polarization is the most important one. It is evaluated by first order perturbation theory and is included in the final results. Other radiative effects are not included in the calculations but a brief description of each of them is given in this chapter.

In Chapter 4, a detailed description of the computer program used in the calculations is given and the method of calculation is outlined. The results of the calculations are also presented in this chapter, using the form of tables and figures.

A method for extracting the nuclear parameters c and t from the experimental energies is described in Chapter 5. The observed transition energies of $(2p_{1/2} - 1s)$, $(3d_{5/2} - 2p_{3/2})$ and $(2s - 2p_{1/2})$ in muonic lead from the work by Anderson et al[3] are used to determine the nuclear parameters for the lead nucleus. The results obtained are given in tables and figures.

In Chapter 6, a summary of the results obtained is given. A brief account of changes which are needed for pionic atoms is also included.

muon in the muonic atom, the main interaction comes from the electrostatic potential produced by the charge distribution inside the nucleus. This suggests we can use the Dirac equation for a central field to describe a muonic atom.

The hamiltonian of the muon can be written as

$$H = -c\vec{\alpha}\cdot\vec{p} - \beta\mu c^2 + V(\vec{r}) \qquad (2.1.2)$$

where $\vec{\alpha}$, β are the Dirac matrices given by

$$\vec{\alpha} = \begin{pmatrix} 0 & \vec{\sigma} \\ \vec{\sigma} & 0 \end{pmatrix} \qquad \beta = \begin{pmatrix} 1 & 0 \\ 0 & -1 \end{pmatrix}$$

with $\vec{\sigma}$ the Pauli spin matrix. μ is the reduced mass of the muon and $V(\vec{r})$ is the electrostatic potential energy of the muon in the field of the nucleus. In equation (2.1.2) only the electrostatic potential is included; other effects, such as vacuum polarization, are small or negligible. They will be discussed later in Chapter 3.

If $\rho(\vec{r})$ denotes the charge distribution of the nucleus and has the normalization

$$\int_0^\infty \rho(\vec{r})\, d^3r = z \qquad (2.1.3)$$

where z is the atomic number of the nucleus, then the electrostatic potential energy $V(\vec{r})$ is given by

$$V(\vec{r}) = -e^2 \int_0^\infty \frac{\rho(\vec{r}')}{|\vec{r} - \vec{r}'|} \, d^3r' \qquad (2.1.4)$$

where e is the electronic charge. The expression (2.1.4) can be expanded in a multipole expansion in terms of spherical harmonics. The first term in the multipole expansion is called the monopole term and is given by the following expression[3]:

$$\phi(r) = -\frac{ze^2}{r} + \frac{4\pi e^2}{r} \int_r^\infty \bar{\rho}(r')(r'^2 - rr') \, dr' \qquad (2.1.5)$$

where $\bar{\rho}(r)$ is called the angular averaged charge distribution and is defined by

$$\bar{\rho}(r) = \frac{1}{4\pi} \int \rho(\vec{r}) \, d\Omega \quad . \qquad (2.1.6)$$

The monopole term has no angular dependence. For a spherically symmetric charge distribution, only the monopole term appears in the multipole expansion.

For a spherically symmetric nucleus, the charge distribution $\rho(\vec{r})$ is angle independent. In this case, the angular averaged charge distribution $\bar{\rho}(r)$ is the same as the charge distribution $\rho(r)$. Using this result, the expression for the monopole term $\phi(r)$ can be rewritten as:

$$\phi(r) = -\frac{ze^2}{r} + \frac{4\pi e^2}{r} \int_r^\infty \rho(r') \, (r'^2 - rr') \, dr' \quad . \qquad (2.1.7)$$

Replacing the electrostatic potential energy $V(\vec{r})$ by

this monopole term, the hamiltonian of the muon in the field of a spherically symmetric nucleus is obtained. The new hamiltonian can be written as

$$H' = -c\vec{\alpha}\cdot\vec{p} - \beta\mu c^2 + \phi(r) \quad . \tag{2.1.8}$$

The Dirac equation that is solved is

$$H'\Psi = E\Psi \tag{2.1.9}$$

where E is the total energy. Equation (2.1.9) describes the muon in a central potential field. It can be separated without approximation in spherical coordinates. Following Schiff[16] and using the operator identity

$$(\vec{\sigma}\cdot\vec{A})(\vec{\sigma}\cdot\vec{B}) = (\vec{A}\cdot\vec{B}) + i\vec{\sigma}\cdot(\vec{A}\times\vec{B}) \tag{2.1.10}$$

where $\vec{\sigma}$ is the Pauli spin matrix and $\vec{A}$ and $\vec{B}$ are any operators which commute with $\vec{\sigma}$, we can write

$$(\vec{\sigma}\cdot\vec{r})(\vec{\sigma}\cdot\vec{L}) = (\vec{\sigma}\cdot\vec{r})[\vec{\sigma}\cdot(\vec{r}\times\vec{p})] = i[(\vec{\sigma}\cdot\vec{r})(\vec{r}\cdot\vec{p}) - r^2(\vec{\sigma}\cdot\vec{p})] \tag{2.1.11}$$

where $\vec{L} = \vec{r}\times\vec{p}$ is the orbital angular momentum. From (2.1.11) we have

$$(\vec{\sigma}\cdot\vec{p}) = \frac{(\vec{\sigma}\cdot\vec{r})}{r^2}\,[(\vec{r}\cdot\vec{p}) + i(\vec{\sigma}\cdot\vec{L})] \tag{2.1.12}$$

Since

$$(\vec{\alpha}\cdot\vec{p}) = \begin{pmatrix} 0 & (\vec{\sigma}\cdot\vec{p}) \\ (\vec{\sigma}\cdot\vec{p}) & 0 \end{pmatrix} ,$$

we have

$$(\vec{\alpha}\cdot\vec{p}) = \alpha_r(p_r + i\frac{(\vec{\sigma}\cdot\vec{L}) + \hbar}{r}) \qquad (2.1.13)$$

where

$$\alpha_r = \frac{\vec{\alpha}\cdot\vec{r}}{r} \qquad (2.1.14)$$

is a hermitian matrix; and

$$p_r = \frac{(\vec{r}\cdot\vec{p}) - i\hbar}{r} = -i\hbar(\frac{\partial}{\partial r} + \frac{1}{r}) \quad . \qquad (2.1.15)$$

We define a new operator k which is related to the total angular momentum by

$$k = \beta(\vec{\sigma}\cdot\vec{L} + \hbar) \quad . \qquad (2.1.16)$$

The hamiltonian H' then becomes

$$H' = c\alpha_r p_r + \frac{i\hbar c}{r}\alpha_r\beta k + \beta\mu c^2 + \phi(r) \qquad (2.1.17)$$

The operator k commutes with the operators β, α_r and p_r and thus also with the whole hamiltonian H', so it is a constant of motion. The eigenvalues of k can be inferred by squaring (2.1.16):

$$\begin{aligned} k^2 &= (\vec{\sigma}\cdot\vec{L})^2 + 2\hbar(\vec{\sigma}\cdot\vec{L}) + \hbar^2 \\ &= (\vec{L} + \frac{1}{2}\vec{\sigma})^2 + \frac{1}{4}\hbar^2 = \vec{J}^2 + \frac{1}{4}\hbar^2 \end{aligned} \qquad (2.1.18)$$

where $\vec{J}^2$ is the operator of the square of angular momentum and has eigenvalues $j(j+1)\hbar^2$. The operator k^2 can have eigenvalues

$$k^2 = j(j+1) + \frac{1}{4} = (j+\frac{1}{2})^2 \quad . \qquad (2.1.19)$$

Hence, the eigenvalue of k can be

$$k = \pm(j+\tfrac{1}{2}) = \pm 1 \ , \ \pm 2 \ , \ . \ . \ . \ . \qquad (2.1.20)$$

The angular and spin parts of the total wave function in equation (2.1. 9) are fixed by the requirement that Ψ be an eigenfunction of the operator k defined by (2.1.16). For such purposes as the computation of energy levels, we need be concerned only with the radial part of the wave function. We are interested in states with well-defined values of the total angular momentum and thus with well-defined values of k. From equation (2.1.17), it follows that the energy of such states can be evaluated from the equation

$$(c\alpha_r p_r + \frac{i\hbar c}{r}\alpha_r \beta k + \beta\mu c^2 + \phi(r) - E)\psi(r) = 0 \qquad (2.1.21)$$

where $\psi(r)$ is the radial part of the total wave function Ψ.

The matrices α_r and β anticommute with each other. We shall choose the representation in which

$$\beta = \begin{pmatrix} 1 & 0 \\ 0 & -1 \end{pmatrix} \quad , \quad \alpha_r = \begin{pmatrix} 0 & -i \\ i & 0 \end{pmatrix} \quad . \qquad (2.1.22)$$

Because of the structure of β and α_r, the radial part of the wave function has two components and is written

$$\psi(r) = \frac{1}{r}\begin{pmatrix} F(r) \\ G(r) \end{pmatrix} \tag{2.1.23}$$

where F and G are called the small and large components respectively and have the normalization

$$\int_0^\infty (F^2 + G^2)\, dr = 1 \quad . \tag{2.1.24}$$

Substituting (2.1.22) and (2.1.23) into (2.1.21) and making use of (2.1.15) the following two coupled differential equations are obtained:

$$\begin{cases} \dfrac{dF(r)}{dr} = \dfrac{kF(r)}{r} - [E - \mu c^2 - \phi(r)]G(r)/\, c \\ \dfrac{dG(r)}{dr} = -\dfrac{kG(r)}{r} + [E + \mu c^2 - \phi(r)]F(r)/\hbar c \end{cases} \tag{2.1.25}$$

with the quantum number k which is related to the orbital and total angular momentum quantum numbers by

$$\begin{aligned} k &= \ell \qquad \text{if} \quad j = \ell - \tfrac{1}{2} \\ k &= -(\ell+1) \qquad \text{if} \quad j = \ell + \tfrac{1}{2} \quad . \end{aligned} \tag{2.1.26}$$

2.2 Dimensionless Formulation for Spherically Symmetric Muonic Atoms

For all the spherically symmetric nuclei considered in this thesis, a two-parameter Fermi-type model is used for the nuclear charge distribution:

$$\rho(r) = \rho_o\{1 + \exp[n(\frac{r}{c} - 1)]\}^{-1} \qquad (2.2.1)$$

where c is the radius at which the charge density is one-half of the central charge density and n is the parameter that determines the shape of the charge distribution. With the normalization for a nucleus of charge z (eqn. (2.1.3)), the central charge density ρ_o (normalization constant of $\rho(r)$) is found to be[3]

$$\rho_o = \frac{3z}{4\pi c^3(1 + \frac{\pi^2}{n^2})} \quad . \qquad (2.2.2)$$

For $n \to \infty$, the Fermi-type model approaches the uniform charge distribution

$$\begin{cases} \rho(r) = \rho_o & r \leq c \\ \rho(r) = 0 & r > c \end{cases} \qquad (2.2.3)$$

Some authors prefer to write the Fermi distribution in terms of the skin thickness t ; i.e. the distance in which the charge density falls from 90% to 10% of its central value. In this case, the Fermi charge distribution is written as

$$\rho(r) = \rho_o \{1 + \exp[4 \ln 3 \ (r-c)/t]\}^{-1} \quad . \qquad (2.2.4)$$

The skin thickness parameter t is related to n and c by the following equation:

$$t = 4 \ln 3 \left(\frac{c}{n}\right) = 4.40\left(\frac{c}{n}\right) \quad . \tag{2.2.5}$$

Using the Fermi-type distribution (2.2.1), the monopole term $\phi(r)$ in (2.1.7) can be written as:

$$\phi(r) = - z e^2 p(r) \tag{2.2.6}$$

where

$$p(r) = \frac{1}{r} - \frac{3}{c^3 r\left(1+\frac{\pi^2}{n^2}\right)} \int_r^\infty \frac{(r'^2 - r'r)}{1+\exp\left[n\left(\frac{r'}{c} - 1\right)\right]} \, dr' \quad . \tag{2.2.7}$$

Substituting (2.2.6) into (2.1.25) we obtain the Dirac equation for a muon in the field of a spherically symmetric nucleus having a Fermi charge distribution:

$$\begin{cases} \dfrac{dF(r)}{dr} = \dfrac{kF(r)}{r} - [E - \mu c^2 + ze^2 p(r)]G(r)/\hbar c \\ \\ \dfrac{dG(r)}{dr} = - \dfrac{kG(r)}{r} + [E + \mu c^2 + zc^2 p(r)]F(r)/\hbar c \quad . \end{cases} \tag{2.2.8}$$

Equations (2.2.8) can be rearranged as

$$\begin{cases} \dfrac{dF(r)}{dr} = \dfrac{kF(r)}{r} - \left[\dfrac{\mu c}{\hbar}\left(\dfrac{E}{\mu c^2} - 1\right) + \dfrac{ze^2}{\hbar c} p(r)\right]G(r) \\ \\ \dfrac{dG(r)}{dr} = - \dfrac{kG(r)}{r} + \left[\dfrac{\mu c}{\hbar}\left(\dfrac{E}{\mu c^2} + 1\right) + \dfrac{ze^2}{\hbar c} p(r)\right]F(r) \quad . \end{cases} \tag{2.2.9}$$

Defining the dimensionless energy $\varepsilon = \frac{E}{\mu c^2}$ where

E is the total energy of the level considered, and

μ is the reduced mass of the muon, and recalling that

$\frac{\hbar}{\mu c} = \lambda\!\!\!^{-}_{\mu}$, the reduced compton wave length of the muon,

and $\frac{e^2}{\hbar c} = \alpha = \frac{1}{137}$, the fine structure constant, we

can write (2.2.8) in a dimensionless form:[14]

$$\begin{cases} \frac{dF(r)}{dr} = \frac{kF(r)}{r} - \left[\frac{1}{\lambda\!\!\!^{-}_{\mu}} (\varepsilon - 1) + z\alpha p(r) \right] G(r) \\ \frac{dG(r)}{dr} = - \frac{kG(r)}{r} + \left[\frac{1}{\lambda\!\!\!^{-}_{\mu}} (\varepsilon + 1) + z\alpha p(r) \right] F(r) \quad . \end{cases} \tag{2.2.10}$$

The dimensionless form is simpler to work with when we solve the Dirac equation numerically.

2.3 Point Nucleus Solution

The simplest assumption we can make about a charge distribution is that all the nuclear charge is concentrated at the center of the nucleus. This is the so called 'point nucleus'. In this case, the electrostatic potential $\phi(r)$ is given by the following expression:

$$\phi(r) = - \frac{ze^2}{r} \quad . \tag{2.3.1}$$

Substituting (2.3.1) into 2.1.25), we get

$$\frac{dF(r)}{dr} = \frac{kF(r)}{r} - (E - \mu c^2 + \frac{ze^2}{r}) G(r)/c$$
$$\frac{dG(r)}{dr} = -\frac{kG(r)}{r} + (E + \mu c^2 + \frac{ze^2}{r}) F(r)/c \quad . \tag{2.3.2}$$

This is the Dirac equation for a muon in the field of a point nucleus; it can be solved analytically (see Appendix B). The total energy E is found to be

$$E = \mu c^2 \left[1 + \left(\frac{z\alpha}{N + \sqrt{k^2 - z^2\alpha^2}} \right)^2 \right]^{-\frac{1}{2}} \quad , \tag{2.3.3}$$

with $k = \pm 1, \pm 2, \ldots$ and $N = 0, 1, 2, \ldots$. The principal quantum number n is related to N by the relation

$$n = N + |k| \quad . \tag{2.3.4}$$

The binding energies of various levels are given by

$$E_b = \mu c^2 - E = \mu c^2 \left\{ 1 - \left[1 + \left(\frac{z\alpha}{N + \sqrt{k^2 - z^2\alpha^2}} \right)^2 \right]^{-\frac{1}{2}} \right\} . \tag{2.3.5}$$

In this work, we are interested in the six lowest levels. The values of k and N for these levels are: 1s ($k=-1$, $N=0$), 2s ($k=-1$, $N=1$), $2p_{1/2}$ ($k=1$, $N=1$), $2p_{3/2}$ ($k=-2$, $N=0$), $3d_{3/2}$ ($k=2$, $N=1$) and $3d_{5/2}$ ($k=-3$, $N=0$). For the lightest nuclei or for the higher levels of the heavy nuclei, it is sufficient to use the point nucleus eigenvalues which are given by (2.3.5). A correction for the effect of finite size of the nucleus may be obtained from a first order perturbation calculation, using the second term in the expression (2.1.7).

However, for most of the cases we are interested in, i.e. the lowest levels in medium or high z nuclei, the Dirac equation (2.2.10) must be solved by numerical integration. The point nucleus solutions obtained above are used as starting values for the trail energies. The detailed procedures for the numerical solution of the Dirac equation are given in Chapter 4.

CHAPTER 3. RADIATIVE CORRECTIONS

The energy eigenvalues which come from the numerical solution of the Dirac equation (2.2.10) do not describe the energy levels of the muonic atom accurately enough, even for a spherically symmetric nucleus. Several radiative corrections must be taken into account.

Among the possible corrections, vacuum polarization is the most important one. It produces an appreciable shift in the energy levels obtained by the numerical calculations. In this thesis, we evaluate these shifts, using a first order perturbation theory and the numerically derived functions. For other radiative corrections such as the muonic Lamb shift, the muon anomalous magnetic moment, the nuclear polarization and the electron screening, no attempt has been made to calculate them. Instead, a brief qualitative description of each one of them is given.

3.1 The Vacuum Polarization Correction

It is predicted by quantum electrodynamics that, in certain respects, the properties of free space are analogous to those of a dielectric medium. The presence of an electrostatic field in free space induces a slight separation of virtual electrons and positrons, which is

referred to as vacuum polarization. It is the most important one among all the possible radiative corrections. While, in the ordinary electronic hydrogen atom, the energy shift due to the effect of vacuum polarization is much smaller than those due to other radiative effects, this is not the case when we deal with muonic atoms. At a distance of the order of the Compton wave length of the electron ($\lambda\!\!\!^{-}_e = \frac{\hbar}{m_e c} \approx 0.386 \times 10^{-10}$ cm), the vacuum polarization of the virtual electrons and positrons leads to an alteration of the electrostatic potential of the nucleus, regardless of what particle, electron or muon, moves around the nucleus. We know that for hydrogen-like atoms, the Bohr orbit is inversely proportional to the mass of the particle, so that the radius of the muon orbit is about 207 times smaller than the radius of the electron orbit and its dimension is of the order of $\sim 10^{-11}$ cm. As a result of this, the muon will spend a greater part of its time in a region where the electrostatic potential of the nucleus is changed by the effect of the vacuum polarization, and which in turn, leads to an appreciable shift of the energy levels. The effect of vacuum polarization has been investigated and calculated by several authors.[3,10,17-20] Glauber et al[17] had developed a set of equations to calculate the first order energy shift due to vacuum polarization for a point-like nucleus. Here we follow quite closely the steps

used by Ford and Wills[10] in the calculation of the vacuum polarization correction.

To the order of the fine structure constant α, and for a general nuclear charge distribution $\rho(\vec{r})$, the vacuum polarization potential energy due to the virtual electron-positron pairs is given by[21,22]

$$V_p(\vec{r}) = -\frac{2\alpha e^2}{3\pi} \int \frac{\rho(\vec{r}')}{|\vec{r}-\vec{r}'|} \chi_1\left(\frac{|\vec{r}-\vec{r}'|}{\lambda\!\!\!^{-}_e}\right) d^3r' \qquad (3.1.1)$$

where $\alpha = \frac{e^2}{\hbar c} = \frac{1}{137}$ is the fine structure constant,

$\lambda\!\!\!^{-}_e = \frac{\hbar}{m_e c}$ is the reduced Compton wavelength of the electron, and $\chi_n(x)$ is the integral given by

$$\chi_n(x) = \int_1^\infty \frac{1}{y^n}\left(1 + \frac{1}{2y^2}\right)\left(1 - \frac{1}{y^2}\right)^{\frac{1}{2}} e^{-2xy}\, dy \quad . \qquad (3.1.2)$$

If the nuclear charge distribution $\rho(r)$ is spherically symmetric, then only the monopole term appears in the multipole expansion of equation (3.1.1). For a Fermi-type charge distribution $\rho(r)$, the vacuum polarization potential energy $V_p(r)$ is given by[23]

$$V_p(r) = \frac{4\alpha e^2}{3\pi r} \int_0^\infty dr' r' \left[H(|r-r'|) - H(r+r')\right] \rho(r') \quad , \qquad (3.1.3)$$

where $H(r)$ is given by

$$H(r) = \frac{1}{2} \lambda\!\!\!^{-}_e \int_e^1 \frac{dy}{y^2} \; e^{-\frac{2yr}{\lambda\!\!\!^{-}_e}} \; (1 + \frac{1}{2y^2})(1 - \frac{1}{y^2}) \quad . \tag{3.1.4}$$

For $r << \lambda\!\!\!^{-}_e$, the asymptotic expansion of the expression (3.1.4) is

$$H(r) - H(0) = r \{\ln(\frac{r\gamma}{\lambda\!\!\!^{-}_e}) - \frac{1}{6} - \frac{3\pi}{8} \frac{r}{\lambda\!\!\!^{-}_e} + \frac{1}{2}(\frac{r}{\lambda\!\!\!^{-}_e})^2 - \frac{\pi}{12}(\frac{r}{\lambda\!\!\!^{-}_e})^3 + O[(\frac{r}{\lambda\!\!\!^{-}_e})^4 \ln(\frac{r}{\lambda\!\!\!^{-}_e})]\} \quad , \tag{3.1.5}$$

where $\ln \gamma = 0.557$ is the Euler's constant.

For a perturbation calculation to first order of $z\alpha$, only the first two terms in equation (3.1.5) are used. In such a case, the vacuum polarization potential energy is given by[10]

$$V_p(r) = \frac{2\alpha}{3\pi} [V_L(r) - \frac{5}{6} \phi(r)] \tag{3.1.6}$$

where $\phi(r)$ is the electrostatic potential energy given in (2.1.7) and $V_L(r)$ is given by

$$V_L(r) = - \frac{2\pi}{r} e^2 \int \rho(r') \, r' \{|r-r'|[\ln \frac{\gamma}{\lambda\!\!\!^{-}_e} |r-r'| - 1] - (r+r')[\ln \frac{\gamma}{\lambda\!\!\!^{-}_e} (r+r') - 1]\} \, dr' \quad , \tag{3.1.7}$$

where $\gamma = 1.781$, and $\rho(r')$ is the nuclear charge distribution. Using the numerically derived normalized wave functions f and g , the energy shift due to vacuum polarization is obtained from a first order perturbation

calculation:

$$\Delta E_p = \int V_p(r)\ (f^2 + g^2)\ dr \quad . \qquad (3.1.8)$$

It is found that the vacuum polarization increases the binding energy of the muon somewhat less than 0.7% . Thus, for the heaviest nuclei, the 1s level vacuum polarization is on the order of 70 KeV . Wichmann and Kroll[20] had estimated the same corrections due to terms in second and higher order in $z\alpha$. They found that the corrections are very small, ($\Delta E_p/E \approx 1.0 \times 10^{-4} \sim 1.5 \times 10^{-4}$) and therefore can often be neglected.

3.2 Brief Description of Other Radiative Corrections

A. The Muonic Lamb Shift and Other Radiative Corrections of Order α

In the Dirac theory for a point-like nucleus, the energies of the $2s_{1/2}$ and $2p_{1/2}$ electronic levels are equal (degenerate). But experiments found that the $2s_{1/2}$ level is actually lower than the $2p_{1/2}$ level. In the case of an ordinary hydrogen atom these two levels are found to be shifted with respect to one another by approximately 10% of the magnitude of the fine structure.

This relative shift of the $2s_{1/2}$ and $2p_{1/2}$ levels is called the Lamb shift and it can be largely accounted for by quantum electrodynamics. It turned out that this shift is basically caused by the interaction of the electron with the vacuum. For muonic atoms, the interaction of the muon with the vacuum will lift the energy levels slightly. Thus the binding energy of the levels of the muonic atom is decreased by this effect.

Barrett et al[23] had estimated the muonic Lamb shift for the lowest levels in muonic bismuth. They found that to about 30% accuracy the shifts for the low-lying states are given by the lowest-order formula:

$$\Delta E_{Ls} = \frac{\alpha}{3\pi\mu^2} \langle\nabla^2 V\rangle [\ln \frac{\mu}{2\Delta\varepsilon} + \frac{11}{24} + \frac{3}{8} - \frac{1}{5}] + \frac{\alpha}{8\pi\mu^2} \langle \frac{2}{r} \frac{dV}{dr} \vec{\sigma}\cdot\vec{L}\rangle \qquad (3.2.1)$$

where $\Delta\varepsilon$ is the average excitation energy of the muon defined by the Bethe sum[43] and μ is the reduced muon mass. They use the binding energy of the muon for a particular energy level to shich the Lamb shift is being calculated for $\Delta\varepsilon$ as an approximation. The 30% uncertainty in the result is mostly due to this approximation. In equation (3.2.1) the $(-\frac{1}{5})$ term corresponds to the vacuum polarization of muon pairs. The $\frac{3}{8}$ and the spin-orbit term correspond to the muon anomalous magnetic moment. The expression $\langle\nabla^2 V\rangle$ is proportional to the probability of overlap of the muon wave function

with the nuclear charge distribution and is given by

$$\langle \nabla^2 V \rangle = 4\pi z\alpha \langle \rho \rangle = 4\pi z\alpha \int \rho(r) \, (f^2 + g^2) \, dr \quad . \qquad (3.2.2)$$

Equation (3.2.1) was evaluated numerically and they found for 1s level, $\Delta E_{Ls} = 3.0 \pm 1.0$ KeV ; for $2p_{1/2}$, $\Delta E_{Ls} = 0.4 \pm 0.3$ KeV ; for $2p_{3/2}$, $\Delta E_{Ls} = 0.7 \pm 0.3$ KeV .

B. Nuclear Polarization Effect

In our calculation for the energy levels of muonic atoms, the muon is treated in the static field of the nucleus, i.e. the nucleus is assumed to be unaffected by the presence of the muon. However, this is not the case in reality. Interactions can arise by the presence of the muon and these interaction may induce changes in or polarize the nucleus. Nuclear polarization is also known as the dispersion effect. The temporary excitation of the nucleus leads to a slight change in the energy levels of the muon. It increases the binding energy by a small amount.

The energy shift due to this effect has been calculated by several authors.[13,35-40] Depending on the nuclear model used, they came up with widely different results. The first estimate was made by Cooper and Henley[13], who have shown that the energy shift due to the

effect of nuclear polarization could be written as

$$\Delta E_{Np}^{(2)} = \sum_{\substack{N,m \\ N\neq 0 \\ m=k}} \frac{\langle \psi_o \phi_R | H' | \psi_N \phi_m \rangle \langle \psi_N \phi_m | H' | \psi_o \phi_k \rangle}{(E_o + \varepsilon_o - E_N - \varepsilon_m)} \qquad (3.2.3)$$

where ψ_o and ψ_N are the initial and intermediate wave functions of the nucleus, ϕ_o and ϕ_m , ϕ_R are the initial and intermediate wave function of the muon, E_o and E_N are the initial and intermediate energies of the nucleus, ε_o and ε_m are the initial and intermediate energies of the muon, and

$$H' = H^e - \langle \psi_o | H^e | \psi_o \rangle \quad , \qquad (3.2.4)$$

with H^e being the electric interaction which is given by

$$H^e = \sum_{i=1}^{Z} \left(\frac{-e^2}{|\vec{r} - \vec{R}_i|} \right) \quad . \qquad (3.2.5$$

Here $\vec{r}$ is the position vector of the negative muon, and $\vec{R}_i$ is the position vector of the i^{th} proton in the nucleus. The superscript (2) in (3.2.3) indicated that the nuclear polarization correction obtained by use of this equation is a second order effect. The first order correction to the total energy of the muon-nucleus system is zero for any muon state. Cooper and Henley[13] crudely estimated the snift for 1s level for several muonic atoms by using

closure over both the nuclear and muon states. They took an average value for the energy denominator and chose the value 13 MeV for $(E_o - E_N)$ from the statistical model. They found that the shifts for the 1s level were: -58 KeV in lead ($_{82}$Pb), -13 KeV in copper ($_{29}$Cu) and -1.2 KeV in aluminum ($_{13}$Al). Lakin and Kohn[37] made an estimate of the same effect and reported a smaller shift. They found that in muonic mercury ($_{80}$Hg), the 1s level shift was -16 ± 8 KeV. They also pointed out that the reduction in the magnitude of the shift was mostly due to the correlated motion of the protons. Chen[38], in his Princeton thesis, repeated Cooper and Henley's calculation with the following two improvements:

1) The intermediate muonic states in the continuum are treated properly.
2) The two nucleon cross terms in the ground state nucleus are included.

He found that the shifts in muonic lead are

$$\Delta E_{N\cdot p} = -6 \pm 0.5 \text{ KeV} \qquad \text{for } 1s$$

$$\Delta E_{N\cdot p} = -1.2 \pm 0.2 \text{ KeV} \qquad \text{for } 2s$$

$$\Delta E_{N\cdot p} = -1.9 \pm 0.2 \text{ KeV} \qquad \text{for } 2p .$$

The nuclear polarization effect was also estimated by Cole[36,39]. He used an average nuclear model and the

experimental inelastic electron scattering cross sections to calculate the shift due to the giant dipole resonance. The results obtained for muonic lead are:

$$\Delta E_{N\cdot p} \approx -6 \text{ KeV} \quad \text{in} \quad 1s$$

and $$\Delta E_{N\cdot p} \approx -2 \text{ KeV} \quad \text{in} \quad 2p \ .$$

Recently, Skardhamar[40] has obtained similar results.

C. Electron Screening Effect

When an atomic electron is within the muon orbit, the effective nuclear charge seen by the muon will be changed. This change in turn will induce a shift in the energy levels of the muon. Since the muon orbits are 207 times smaller than their corresponding electron orbits, the main contribution to this effect comes from the K-shell electrons. The electron screening effect has been calculated by Barrett et al[23]. They found that the shifts in the energy levels of muonic bismuth ($_{83}$Bi) vary from 4.6 eV for the 1s state to 190 eV for the 5g states. The electron screening becomes more important as the level goes higher. For the lowest levels which we are interested in, the corrections are of the order of a few eV . Electron screening increases the transition energies.

CHAPTER 4.

NUMERICAL METHODS FOR THE CALCULATION OF ENERGY LEVELS

The energy levels of the muon in the field of a Fermi-type charge distribution are obtained by the numerical solutions of the dimensionless equations (2.2.10). A computer program has been developed for this purpose. In this chapter, first a description is given of the computer program and the procedures are outlined for calculating the energy levels and also their corresponding vacuum polarization corrections. Then, in the second part, the results of the calculation for the lowest six levels (1s, 2s, $2p_{1/2}$, $2p_{3/2}$, $3d_{3/2}$ and $3d_{5/2}$) of the muonic atoms are presented, in the form of tables. In Table 4.2.1 , the mass number A , the nuclear parameters c and n , the calculated binding energies of the levels considered and their corresponding vacuum polarization corrections are tabulated, in increasing order of z . In Table 4.2.2, several energy differences between two levels are listed. These include the $2p_{3/2} - 2p_{1/2}$ splitting and the transitions $2p_{3/2} - 1s$, $3d_{5/2} - 2p_{3/2}$, $2s - 2p_{1/2}$, and $3d_{1/2} - 2s$. In the same table, we also list the experimental values for some transitions as a comparison with the calculated results. The Fermi-type charge distribution, as well as the numerically derived potentials, and the normalized wave

functions for lead ($_{82}Pb$) are shown graphically in figures 4.2.1 to 4.2.5 . A complete listing of the computer program for the calculation is given in Appendix D .

4.1 Detailed Calculation Procedures

In the computer program which has been developed to calculate the energy levels of the muonic atoms, the electrostatic potential of the nuclear charge distribution and the effective potential due to vacuum polarization are first evaluated. This is because these two potentials are functions of the quantities z, c and n which are constant for a particular atom. This means that these two potentials are the same for all muonic levels in this particular atom and therefore they only have to be evaluated once when the various energy levels and their corresponding vacuum polarization corrections are calculated. Throughout the calculation a two-parameter Fermi-type charge distribution is used. This distribution is characterized by the radial parameter c , and the surface thickness parameter n or the skin thickness parameter t . (See Section 2.2 .) These parameters, for some nuclei, have been determined by Hofstadter[9] in high energy electron scattering experiments. On averaging these experimental values, it was found that the skin thickness parameter t was approximately the same for all nuclei except the

lightest ones[11,41] and it was given by

$$t = 2.4 \times 10^{-13} \text{ cm} \quad . \tag{4.1.1}$$

The dependence of the radial parameter c on A was

$$c \simeq 1.08\ A^{1/3} \times 10^{-13} \text{ cm} \tag{4.1.2}$$

where A is the atomic mass number of the natural isotope mixture.

In the calculation, except for some cases, the nuclear parameters given by (4.1.1) and (4.1.2) are used for all nuclei considered. The exceptions are the ones whose nuclear parameters have been determined directly by the electron scattering experiments. In particular, the values of c and t for nuclei $_{20}Ca$, $_{23}Va$, $_{27}Co$, $_{28}Ni$, $_{49}In$, $_{51}Sb$, $_{79}Au$ and $_{83}Bi$ are taken from the experimental results of Hofstadter[9] while the same values for the lightest nuclei $_{3}Li$, $_{4}Be$, $_{5}B$, $_{6}C$, $_{7}N$ and $_{8}O$ are taken from the results of Meyer-Birkhout et al[15].

The electrostatic potential produced by a Fermi-type charge distribution is given by equation (2.2.6). It cannot be expressed explicitly in an analytical form and thus must be evaluated numerically. To this end, the well-known Simpson's rule for the approximation solution of a definite integral is used. The potential is calculated for a series of values of r, the radial variable. The

calculation is started at $r_o = 0.001$ fm , (1 fm = 10^{-13}cm), an arbitrarily chosen point that is close to zero. The second value of r is set equal to $r_o + h = r_1$, and the third value of r is set equal to $r_o + 2h = r_1 + h = r_2$ etc; here h is a constant which is set equal to 0.25 fm. For each value of r , the integration over r' in (2.2.7) has to be done once and is calculated by means of Simpson's rule. It is found that when $r = 30$ fm , the contribution from the second term in (2.2.7) is very small and negligible. This means that the electrostatic potential is practically the same as the one produced by a point-like nucleus for such a large value of r .

The effective potential due to vacuum polarization given by equation (3.1.6) is calculated next. Simpson's rule is also used to evaluate $V_L(r)$, given by (3.1.7) . The step size in the integration is chosen to be the same as the one used in the calculation of $V(r)$. It is found that without loss of any significant contribution, the upper limit of the integral in (3.1.7) can be set equal to 30 fm , i.e. the integration over r' runs from $r' = 0$ to $r' = 30$ fm .

After the electrostatic potential and the vacuum polarization correction potential are obtained, the energy levels of the muonic atom are then calculated. Following Acker et al[28], the Dirac equations are solved

numerically, treating the dimensionless energy ε as the eigenvalue. Both of the Dirac equations for a point-like nucleus and for a finite-size nucleus with a Fermi-type charge distribution are solved. At a certain distance away from the center of the nucleus, called the matching radius, these solutions are compared. An interpolation program enables one to find the correct energy eigenvalues.

The Dirac equation for a point-like nucleus is given by (2.3.2) . They can perhaps be solved analytically, but we have not tried to do so. Instead, they are solved numerically in a computer. For such a purpose, the fourth-order Runge-Kutta method is used. This method is most commonly used in the numerical solution of a first-order ordinary differential equation. Its application is readily extended to the problem of solving a first-order system of two equations. The formulae of the fourth-order Runge-Kutta method are given in Appendix C .

The numerical solutions of the Dirac equation for a point-like nucleus are begun at $r_o = 0.001$ fm (the same point where the calculation of $\phi(r)$ is started). The initial values of F and G at this

point are obtained from the aymptotic solutions of equation (2.3.2). There are two sets of solutions[14], depending on the sign of the quantum number k. For k greater than zero, the asymptotic solutions are:

$$F = A \frac{2k + 1}{(1+\varepsilon)/\lambda\!\!\!^{-}_{\mu} + \alpha z \phi(0)} r^{k}$$

$$G = A\, r^{k+1} \qquad (4.1.3)$$

and for k less than zero,

$$F = -B \frac{\alpha z \phi(0) + (\varepsilon-1)/\lambda\!\!\!^{-}_{\mu}}{1 - 2k} r^{1-k}$$

$$G = B\, r^{-k} \qquad (4.1.4)$$

where $\phi(0)$ is the electrostatic potential at $r = r_o$, $\lambda\!\!\!^{-}_{\mu}$ is the reduced Compton wavelength of the muon, and A, B are arbitrary constants.

For the sake of simplicity, A and B are chosen to be unity in our calculations. The quantity $\phi(0)$ is given by $\phi(r_o) = -\frac{ze^2}{r_o}$. The energy eigenvalue ε

is obtained from the formula (2.3.5) in Section 2.3 . Using the initial values of F and G thus obtained and with the help of the fourth-order Runge-Kutta method, the values of the radial wave functions F and G at $r_1 = r_o + h$ are calculated. Here h is the step size of the integration and is chosen to be equal to 0.25 fm . The solutions of F and G at r_1 are then used as the initial values for the next calculation of F and G at $r_2 = r_1 + h$ . . . . and so on. In this way, the repeated application of the fourth-order Runge-Kutta method permitted the values of F and G at $r_i = r_{i-1} + h$, $i = 1, 2, 3 \ldots$ to be obtained. The integrations are continued until r reaches the matching radius.

The program is then moved to the solution of the Dirac equations for a finite nucleus with a Fermi-type charge distribution. The procedures for the solutions of F and G are essentially the same as in the calculations of a point-like nucleus. The initial values of F and G are also obtained from (4.1.3) or (4.1.4), except in this case, the first value found in the numerical calculation of the electrostatic potential $\phi(r)$ is used for $\phi(0)$. The integrations of F and G for a finite nucleus are also started at $r_o = 0.001$ fm and the step size h is chosen to be the same as the one used in the point nucleus

calculations. (This choice is necessary because the results of the point nucleus and finite nucleus calculations are compared at the matching radius.) The trial energy eigenvalue ε is first set equal to ε_1, the point-like nucleus value and the Dirac equations are solved by the same method used previously. The integrations are stopped when r reaches the matching radius. A comparison of the solutions of the Dirac equations for a point-like and a finite size nucleus is made at this point by calculating the difference D_1 given by the following equation:

$$D_1 = F_i(\varepsilon_1)G_o(\varepsilon_1) - F_o(\varepsilon_1)G_i(\varepsilon_1) \qquad (4.1.5)$$

where F_o, G_o and F_i, G_i are the values of the radial wave functions of a point-like nucleus and a finite-size nucleus at the matching radius respectively.

Similarly, two more differences D_2 and D_3 are obtained by repeating the solution of Dirac equations twice, with two different trial eigenvalues ε_2 and ε_3:

$$\varepsilon_2 = \varepsilon_1 + \Delta\varepsilon$$

$$\varepsilon_3 = \varepsilon_2 + \Delta\varepsilon = \varepsilon_1 + 2\Delta\varepsilon \qquad (4.1.6)$$

where $\Delta\varepsilon$ is the change in the dimensionless energy and is roughly scaled to the expected difference between the point nucleus energy and the actual energy.

Using this set of trial energy eigenvalues ε_1, ε_2, ε_3 and their corresponding differences D_1, D_2, D_3 a new trial eigenvalue ε' can be found for which the difference D' is equal to zero. This is done using the Lagrange interpolation formula; i.e., by first calculating the quantities ε_{12} and ε_{13} :

$$\varepsilon_{12} = (D_2\varepsilon_1 - D_1\varepsilon_2)/(D_2 - D_1) \qquad (4.1.7)$$

$$\varepsilon_{13} = (D_3\varepsilon_1 - D_1\varepsilon_3)/(D_3 - D_1) \quad . \qquad (4.1.8)$$

The required eigenvalue ε' is then given by

$$\varepsilon' = (D_3\varepsilon_{12} - D_2\varepsilon_{13})/(D_3 - D_2) \quad . \qquad (4.1.9)$$

Starting from the solution of the Dirac equation for a finite nucleus, the above procedures are then repeated. The eigenvalue ε' obtained from the interpolation is used as the first trial energy eigenvalue. The second and third trial eigenvalues are set equal to $\varepsilon' - \Delta\varepsilon'$ and $\varepsilon' - 2\Delta\varepsilon'$ with $\Delta\varepsilon' = \frac{1}{5}\Delta\varepsilon$. This new set of energy eigenvalues and their corresponding D's, together with equations (4.1.7), (4.1.8) and (4.1.9) enable one to find another new eigenvalue ε'' for which the difference D'' is equal to zero. ε'' is closer to the correct energy eigenvalue than ε' . This iteration scheme is continued until the difference between two successive trial eigenvalues is less than 1.0×10^{-8}

(i.e. the energy difference between these two successive trials is less than about 1 eV) The correct energy eigenvalue is then given by the last trial eigenvalue. If ε_c denotes this correct energy eigenvalue, the binding energy of the particular muonic level considered is given by

$$E_{b.E.} = \mu c^2 (1 - \varepsilon_c) \tag{4.1.10}$$

where μ is the reduced mass of the muon.

In the present calculation, the muon mass assumed is[42]

$$m_\mu = 206.84\ m_e = 105.69\ \text{MeV} \tag{4.1.11}$$

and the reduced mass of the muon in a particular atom is given by

$$\mu = \frac{A \cdot m_\mu}{A + 0.1135} \tag{4.1.12}$$

where A is the mass number of the atom. (0.1135 is the ratio of the muon mass to the mass of a nucleon.)

For the lightest nuclei, the matching radius is set equal to the value r = 50 fm. As the atomic number z increases, the radius of the orbit of a certain muonic level decreases. This means that a smaller matching radius can be used as our calculation of the energies go on, in the increasing order of z . For the heaviest

nuclei, the solutions of the Dirac equations for a point-like nucleus and for a finite nucleus were compared at $r = 30$ fm .

Using the correct energy eigenvalue found above, the finite nucleus Dirac equations are solved once more. In this way, the unnormalized radial wave functions F and G are obtained. These wave functions, after being normalized, were used in the calculation of the vacuum polarization correction. If f and g are the normalized wave functions, then the wave functions F and G can be written as

$$\begin{cases} F = Nf \\ G = Ng \end{cases} \tag{4.1.13}$$

where N is the normalization constant. From equation (4.1.13) and the normalization condition:

$$\int (f^2 + g^2)\, dr = 1 \quad , \tag{4.1.14}$$

we have

$$\int (F^2 + G^2)\, dr = N^2 \int (f^2 + g^2)\, dr = N^2 \tag{4.1.15}$$

The normalization constant N can be found by evaluating the integral in (4.1.15). In our program, this integral is evaluated numerically by means of Simpson's rule. The starting point and the step size of the integration are predetermined. They are restricted to take the same values used previously.

The last step in the calculation is the evaluation of the energy shift due to the effect of vacuum polarization. This correction, considered to be the most important one among all radiative corrections, is given by (3.1.8) in first-order perturbation theory. Simpson's rule is used again to evaluate the integral in (3.1.8). The normalized wave functions obtained above are used and the effective potential of this correction $V_p(r)$ has been found earlier. The same starting point and step size as in the previous calculation are used. The integration over r is done up to 50 fm . It is found that for nuclei with atomic number z up to 9 , the vacuum polarization corrections for the 2p and 3d levels are very small and therefore can be ignored.

To sum up, the detailed procedures in our calculation for the energy levels of the muonic atom can be outlined as follows:

1) The electrostatic potential $\phi(r)$ and the effective potential due to vacuum polarization are first evaluated by means of Simpson's rule. These two potentials are the same for all levels in a particular atom.

2) Using the fourth-order Runge-Kutta method, the Dirac equations for a point-like nucleus are solved.

3) The Dirac equations for a finite nucleus are solved by the same method used in (2). At the matching radius, the solutions obtained in this step and the ones obtained in (2) are compared by calculating the difference $D = F_i G_o - F_o G_i$.

4) The eigenvalue ε in the Dirac equations is then changed to $\varepsilon - \Delta\varepsilon$ and $\varepsilon - 2\Delta\varepsilon$, and step (3) is repeated twice.

5) Using the trial eigenvalues ε_1, ε_2, ε_3 and the results D_1, D_2, D_3 obtained in (3) and (4) and an interpolation program, a new eigenvalue for which $D = 0$ is found.

6) The result obtained in (5) is then used as the first trial eigenvalue for the Dirac equations and steps (3), (4), (5) are repeated. A new eigenvalue is found. This new eigenvalue is closer to the correct eigenvalue than the previous one. This iteration scheme is continued until the difference between two successive trial eigenvalues is less than 1.0×10^{-8} . When the iteration is stopped, the correct eigenvalue is found.

7) Using the correct eigenvalue found in (6), the unnormalized wave functions F and G are obtained by solving the Dirac equations once more.

8) By means of Simpson's rule, the functions F and G obtained in (7) are first normalized and then the vacuum polarization correction evaluated.

The program is run in the University of Victoria IBM 360-50 computer. The storage needed for the program is 66K. The computing time for each run is about 10 minutes.

4.2 Results of the Calculation

In this section, the results obtained in the above calculation are presented. In Table 4.2.1 the mass number A , the nuclear parameters c and n and the binding energies of the six lowest levels considered for each muonic atom are listed. There are two columns for each level in this table; the first one shows the calculated binding energy (including the vacuum polarization correction) while the second one shows the energy shift due to vacuum polarization in that level. In Table 4.2.2 , several transition energies among the levels considered are listed. For some transitions, experimental values with references are also listed for a comparison with our results. Typical results are shown graphically for lead in figures 4.2.1 to 4.2.5 . The Fermi-type nuclear charge distribution is shown in figure 4.2.1 , the electrostatic potential $\phi(r)$ in figure 4.2.2 , and the normalized wave functions of all six levels in figures 4.2.3 , 4.2.4 , and 4.2.5 .

Z	Element	Mass	Nuclear Parameters		Binding Energies and Vacuum Polarization Correction in KeV											
					1s		2s		$2p_{1/2}$		$2p_{3/2}$		$3d_{3/2}$		$3d_{5/2}$	
		A	c (fm)	n	B.E.	V.P.	B.E.	V.P.	B.E.	V.P.	B.E.	V.P.	B.E.	V.P.	B.E.	V.P.
3	Li	6.94	1.20	1.71	25.452	0.062	5.684		6.225		6.224		2.768		2.768	
4	Be	9.01	0.9	1.14	44.473	0.091	9.962		11.141		11.139		4.940		4.939	
5	B	10.81	2.0	3.64	69.589	0.235	16.219		17.403		17.397		7.735		7.734	
6	C	12.01	2.24	4.48	100.176	0.325	23.428		25.137		25.125		11.149		11.148	
7	N	14.01	2.30	4.60	136.241	0.508	32.235		34.199		34.176		15.196		15.194	
8	O	16.0	2.60	6.02	178.034	0.734	42.574		44.797		44.758		19.869		19.865	
9	F	19.0	2.88	5.28	224.772	1.017	51.284		56.583		56.521		25.177		25.171	
11	Na	23.0	3.07	5.63	334.476	1.668	71.778	0.204	84.739	0.152	84.602	0.150	37.655	0.020	37.642	0.020
12	Mg	24.3	3.13	5.74	396.303	2.038	84.642	0.376	101.038	0.200	100.847	0.201	44.829	0.038	44.810	0.037
13	Al	27.0	3.24	5.94	464.235	2.573	98.624	0.403	119.167	0.276	118.873	0.270	52.641	0.042	52.614	0.041
14	Si	28.1	3.26	6.02	535.621	2.947	112.094	0.435	137.131	0.342	136.756	0.336	61.065	0.058	61.028	0.056
15	P	31.0	3.39	6.22	609.868	3.621	125.665	0.607	155.670	0.403	155.173	0.395	70.139	0.079	70.074	0.077
16	S	32.1	3.43	6.29	693.303	4.124	144.359	0.667	179.558	0.445	178.956	0.434	79.823	0.081	79.762	0.079
17	Cl	35.5	3.55	6.51	776.461	4.596	161.214	0.815	202.123	0.603	201.337	0.592	90.150	0.116	90.079	0.114
19	K	39.1	3.67	6.72	965.233	5.954	209.019	1.014	255.715	0.796	254.509	0.781	112.678	0.169	112.557	0.165
20	Ca	40.1	3.64	6.41	1063.96	6.624	227.712	1.236	283.020	0.825	281.525	0.803	124.870	0.188	124.720	0.184
21	Sc	45.0	3.84	7.04	1166.35	7.463	249.293	1.415	311.246	0.896	309.521	0.872	137.735	0.196	137.554	0.193
22	Ti	47.9	3.92	7.19	1270.66	8.014	271.036	1.506	342.192	1.060	339.996	1.031	151.210	0.202	150.994	0.199
23	Va	50.9	4.00	7.33	1377.86	8.825	289.277	1.741	369.235	1.190	366.686	1.155	165.332	0.278	165.074	0.272
24	Cr	52.0	4.03	7.39	1491.90	9.576	317.865	1.924	405.743	1.332	402.767	1.289	180.070	0.317	179.761	0.311

TABLE 4.2.1 Calculated energies of the six lowest levels in muonic atoms.

Z	Element	Mass	Nuclear Parameters		Binding Energies and Vacuum Polarization Correction in KeV											
					1s		2s		$2p_{1/2}$		$2p_{3/2}$		$3d_{3/2}$		$3d_{5/2}$	
		A	c (fm)	n	B.E.	V.P.	B.E.	V.P.	B.E.	V.P.	B.E.	V.P.	B.E.	V.P.	B.E.	V.P.
25	Mn	54.9	4.11	7.53	1608.173	10.463	342.467	1.992	441.878	1.486	438.282	1.435	195.456	0.384	195.094	0.377
26	Fe	55.8	4.13	7.57	1729.78	11.247	370.812	2.014	479.286	1.652	475.190	1.591	211.463	0.392	211.042	0.385
27	Co	58.9	4.09	7.17	1850.80	12.154	399.188	2.112	517.094	1.832	512.540	1.760	228.123	0.401	227.629	0.394
28	Ni	58.7	4.30	7.59	1973.17	13.074	429.751	2.231	559.505	2.024	554.193	1.941	245.397	0.412	244.826	0.404
29	Cu	63.6	4.31	7.90	2101.48	13.974	456.981	2.452	597.579	2.232	591.448	2.134	263.346	0.476	262.688	0.467
30	Zn	65.4	4.35	7.98	2233.31	14.839	490.614	2.646	642.942	2.453	636.021	2.340	281.908	0.536	281.154	0.527
31	Ga	69.7	4.45	8.15	2363.01	15.746	519.559	2.831	683.865	2.688	676.011	2.559	301.132	0.602	300.272	0.593
32	Ge	72.6	4.51	8.26	2498.45	16.688	552.648	3.204	729.226	2.938	720.413	2.790	320.987	0.628	320.010	0.618
33	As	74.9	4.55	8.35	2638.41	17.597	586.933	3.427	776.059	3.203	766.217	3.034	341.480	0.694	340.374	0.683
34	Se	79.0	4.63	8.50	2781.18	18.562	621.120	3.631	823.457	3.482	812.424	3.291	362.630	0.765	361.382	0.753
35	Br	79.9	4.65	8.53	2903.78	19.547	657.278	3.894	872.303	3.777	860.049	3.561	384.402	0.829	383.001	0.815
37	Rb	85.5	4.76	8.72	3207.73	21.713	739.983	4.259	978.352	4.410	963.491	4.141	429.907	0.964	428.154	0.945
38	Sr	87.6	4.80	8.79	3361.96	22.604	786.418	4.376	1037.56	4.750	1021.32	4.450	453.629	1.031	451.677	1.011
39	Y	88.9	4.82	8.84	3517.26	23.493	835.650	4.427	1098.25	5.105	1080.562	4.773	478.001	1.103	475.834	1.080
40	Zr	91.2	4.86	8.91	3672.51	24.385	884.820	4.677	1159.31	5.474	1140.19	5.109	503.060	1.379	500.617	1.353
41	Nb	92.9	4.89	8.97	3791.77	25.656	932.509	4.829	1208.48	5.958	1187.22	5.581	528.692	1.643	526.041	1.612
42	Mo	96.0	4.95	9.07	3969.72	27.175	973.696	5.180	1274.16	6.342	1250.60	5.928	555.073	1.729	552.152	1.695
43	Tc	99.0	5.00	9.16	4129.07	28.214	1032.890	5.476	1336.99	6.741	1311.36	6.289	582.064	1.819	578.852	1.781
44	Ru	101.1	5.03	9.22	4283.67	29.293	1080.89	5.859	1394.27	7.159	1366.54	6.664	609.806	2.012	606.255	1.970
45	Rh	102.9	5.06	9.28	4442.63	30.376	1136.06	6.147	1461.04	7.588	1431.19	7.052	638.123	2.108	634.321	2.063
46	Pd	106.4	5.12	9.38	4602.78	31.487	1187.31	6.594	1528.02	8.033	1495.54	7.453	667.089	2.209	662.939	2.159

TABLE 4.2.1 - continued

Z	Element	Mass	Nuclear Parameters		Binding Energies and Vacuum Polarization Correction in KeV											
					1s		2s		$2p_{1/2}$		$2p_{3/2}$		$3d_{3/2}$		$3d_{5/2}$	
		A	c (fm)	n	B.E.	V.P.	B.E.	V.P.	B.E.	V.P.	B.E.	V.P.	B.E.	V.P.	B.E.	V.P.
47	Ag	107.9	5.14	9.43	4763.67	32.495	1241.55	6.831	1593.82	8.496	1558.06	7.869	696.704	2.313	692.179	2.258
48	Cd	112.4	5.21	9.56	4919.32	33.387	1293.46	7.235	1661.50	8.969	1622.95	8.295	726.997	2.422	722.074	2.362
49	In	114.8	5.24	10.02	5084.22	34.298	1352.50	7.535	1732.48	9.471	1691.84	8.742	757.951	2.635	752.599	2.570
50	Sn	118.7	5.31	9.73	5231.65	35.294	1411.87	7.826	1804.86	9.932	1761.40	9.213	789.675	2.826	783.755	2.758
51	Sb	121.8	5.32	9.36	5394.01	36.304	1457.24	8.109	1880.67	10.476	1834.84	9.651	821.835	2.975	815.558	2.897
52	Te	127.6	5.44	9.97	5556.80	37.392	1503.68	8.437	1956.754	11.108	1907.60	10.293	854.900	3.290	848.055	3.200
53	I	126.9	5.43	9.95	5717.07	38.486	1553.26	8.726	2032.23	11.923	1979.79	11.015	888.400	3.528	881.047	3.436
55	Cs	132.9	5.51	10.10	6043.37	40.616	1670.25	9.560	2193.65	12.798	2137.83	11.782	957.651	4.006	949.151	3.893
56	Ba	137.4	5.57	10.22	6228.15	41.684	1728.48	9.859	2275.36	13.363	2212.90	12.291	993.572	4.153	984.435	4.032
57	La	138.9	5.59	10.25	6380.22	42.693	1785.01	10.124	2355.17	13.954	2289.22	12.819	1029.60	4.304	1019.79	4.173
58	Ce	140.1	5.61	10.24	6559.84	43.713	1846.18	10.417	2438.68	14.561	2369.18	13.361	1066.58	4.461	1056.07	4.321
59	Pr	140.9	5.62	10.30	6701.85	44.625	1907.52	10.728	2528.50	15.184	2455.40	13.916	1104.25	4.622	1092.98	4.471
60	Nd	144.3	5.67	10.39	6890.23	45.584	1971.27	11.128	2616.49	15.805	2538.98	14.475	1142.60	4.788	1130.55	4.626
61	Pm	145.0	5.67	10.40	7038.40	46.498	2033.23	11.463	2702.65	16.456	2621.22	15.055	1181.63	4.959	1168.76	4.785
62	Sm	150.4	5.74	10.53	7189.62	47.484	2095.76	11.753	2787.46	17.087	2702.25	15.628	1221.36	5.185	1207.62	4.997
63	Eu	152.0	5.76	10.57	7341.95	48.447	2157.63	12.107	2873.29	17.755	2784.27	16.227	1261.76	5.367	1247.12	5.186
64	Gd	157.3	5.83	10.69	7495.89	49.323	2221.02	12.732	2961.11	18.405	2867.79	16.819	1302.86	5.654	1287.14	5.336
65	Tb	158.9	5.85	10.72	7651.77	50.215	2285.80	13.295	3050.46	19.096	2952.83	17.438	1344.65	5.776	1328.05	5.549
66	Dy	162.5	5.89	10.81	7809.59	51.098	2351.97	13.744	3141.52	19.780	3039.39	18.058	1387.12	5.995	1369.49	5.752
67	Ho	164.9	5.92	10.86	7969.35	51.984	2419.53	14.211	3233.99	20.486	3127.47	18.694	1430.29	6.291	1411.57	6.031
68	Er	167.3	5.95	10.91	8131.05	52.876	2488.48	14.687	3327.99	21.214	3217.07	19.385	1474.98	6.587	1454.35	6.326

TABLE 4.2.1 - continued

Z	Element	Mass	Nuclear Parameters		Binding Energies and Vacuum Polarization Correction in KeV											
					1s		2s		$2p_{1/2}$		$2p_{3/2}$		$3d_{3/2}$		$3d_{5/2}$	
		A	c (fm)	n	B.E.	V.P.	B.E.	V.P.	B.E.	V.P.	B.E.	V.P.	B.E.	V.P.	B.E.	V.P.
69	Tm	168.9	5.97	10.95	8294.69	53.762	2558.82	15.120	3423.52	22.038	3308.19	20.048	1519.84	6.828	1498.53	6.531
70	Yb	173.0	6.02	11.03	8460.27	54.713	2630.55	15.681	3520.90	22.755	3400.83	20.702	1569.63	7.151	1547.54	6.835
71	Lu	175.0	6.04	11.08	8627.79	55.602	2703.67	16.164	3620.21	23.505	3494.99	21.387	1616.57	7.481	1592.20	7.144
72	Hj	178.5	6.08	11.15	8797.25	56.493	2778.18	16.423	3720.52	24.243	3590.67	22.052	1663.20	7.717	1638.51	7.359
73	Ta	181.0	6.11	11.20	8968.65	57.365	2854.08	16.814	3822.50	25.292	3687.87	22.987	1710.23	8.062	1684.33	7.680
74	W	183.9	6.14	11.26	9141.99	58.384	2931.37	17.206	3926.30	26.302	3786.59	24.081	1758.25	8.312	1730.92	7.906
75	Re	186.2	6.17	11.31	9317.27	59.392	3010.05	17.676	4032.04	27.329	3886.83	25.187	1807.99	8.669	1778.17	8.238
76	Os	190.2	6.21	11.39	9494.49	60.415	3090.12	17.987	4139.11	28.086	3988.59	25.834	1857.40	8.924	1826.05	8.465
77	Ir	192.2	6.23	11.43	9673.65	61.426	3171.76	18.192	4247.30	28.752	4091.87	26.485	1907.55	9.185	1875.59	8.692
78	Pt	195.1	6.26	11.48	9854.75	62.398	3254.61	18.375	4357.69	29.427	4196.67	27.128	1958.40	9.436	1924.78	8.916
79	Au	197.0	6.38	12.10	10037.79	63.404	3338.85	18.569	4469.57	30.129	4302.99	27.779	2010.87	9.694	1974.57	9.142
80	Hg	201.0	6.33	11.60	10222.77	64.625	3424.48	18.863	4583.05	30.847	4410.83	28.436	2063.49	9.958	2025.21	9.383
81	Tl	204.4	6.36	11.66	10409.69	66.893	3511.50	19.021	4699.37	31.540	4520.19	28.724	2116.19	10.214	2077.23	9.615
82	Pb	207.2	6.71	14.00	10598.37	67.103	3599.91	19.324	4817.02	32.317	4631.07	29.792	2172.31	10.487	2130.02	9.852
83	Bi	209.0	6.47	10.54	10789.17	67.846	3689.71	19.538	4932.92	32.967	4743.47	30.482	2226.75	10.695	2183.01	10.104
84	Po	210.0	6.42	11.77	10979.15	68.534	3778.86	19.543	5046.05	33.502	4853.83	31.184	2278.94	11.024	2234.42	10.411
85	At	215.0	6.47	11.86	11171.04	69.246	3869.23	19.847	5160.99	34.642	4965.40	31.903	2333.43	11.405	2286.62	10.722
87	Fa	223.0	6.55	12.01	11501.82	70.642	4047.97	20.334	5389.98	35.819	5185.54	33.196	2449.97	12.115	2399.25	11.395
88	Ra	226.0	6.58	12.06	11679.38	71.354	4142.45	20.652	5509.43	36.657	5301.82	33.904	2505.14	12.478	2452.17	11.653
90	Th	232.0	6.64	12.17	11979.94	72.695	4332.93	21.158	5720.69	38.312	5504.10	35.614	2628.32	13.165	2559.77	12.314
92	U	238.0	6.69	12.27	12311.33	74.358	4513.41	22.894	5955.11	39.673	5727.69	36.887	2763.13	14.029	2686.56	13.137

TABLE 4.2.1 - continued

Element	$2p_{3/2} - 1s$			$2p_{3/2} - 2p_{1/2}$			$3d_{5/2} - 2p_{3/2}$			$2s - 2p_{1/2}$	$3d_{3/2} - 2s$
	calculated	experiment	ref.	calculated	experiment	ref.	calculated	experiment	ref.	calculated	calculated
$_{3}Li$	19.228			0.001			3.456			0.540	2.916
$_{4}Be$	33.334			0.002			6.200			1.177	5.022
$_{5}B$	52.192	52.23±0.15	24	0.006			9.663			1.378	8.284
$_{6}C$	75.051	75.25±0.15	24	0.012			13.977			1.697	12.279
$_{7}N$	102.065	102.21±0.15	24	0.023			18.982			1.941	17.039
$_{8}O$	133.276	133.56±0.15	24	0.039			24.893			2.184	22.705
$_{9}F$	168.251	168.45±0.15	24	0.062			31.350			5.237	26.107
$_{11}Na$	249.874	250.21±0.15	24	0.137			46.960			12.824	34.136
$_{12}Mg$	295.456	296.55±0.15 295.6 ± 1.6	24 25	0.191			56.037			16.205	39.813
$_{13}Al$	345.362	346.82±0.15 345.7 ± 1.2 350.0	24 25 13	0.294			66.259			20.249	45.983

TABLE 4.2.2 Energy differences of muonic atoms in KeV

Element	$2p_{3/2} - 1s$			$2p_{3/2} - 2p_{1/2}$			$3d_{5/2} - 2p_{3/2}$			$2s - 2p_{1/2}$	$3d_{3/2} - 2s$
	calculated	experiment	ref.	calculated	experiment	ref.	calculated	experiment	ref.	calculated	calculated
$_{14}Si$	398.865	400.22±0.15 400.4±1.3 400.2±0.6	24 25 26	0.375			75.728			24.662	51.029
$_{15}P$	454.695	456.54±0.20 458.5±1.3	24 25	0.497			85.099			29.308	55.726
$_{16}S$	514.347	516.24±0.25 517.2±3 522.0±1.2	24 27 25	0.602			99.194			34.597	64.536
$_{17}Cl$	575.124	578.56±0.30 578.6±1.5 582.8±1.3	24 28 25	0.786			111.258			40.123	71.058
$_{19}K$	710.724	714±3 714.1±4.0 712.64±0.23	29 27 26	1.206			141.952			48.490	93.341
$_{20}Ca$	782.435	783.8±1.5 783.56±0.16 782.8±3.0	28 26 27	1.495			156.805			53.813	102.842
$_{21}Se$	856.829			1.725			171.967			60.228	111.739
$_{22}Ti$	930.664	932.5±5.0 924.7±2.5 937±7	27 30 29	2.196			189.002			68.960	119.826
$_{23}Va$	1011.17			2.549			201.612			76.409	128.945
$_{24}Cr$	1089.13	1094±4	31	2.976			223.006			84.901	137.790

TABLE 4.2.2 - continued

Element	$2p_{3/2}$ - 1s			$2p_{3/2}$ - $2p_{1/2}$			$3d_{5/2}$ - $2p_{3/2}$			2s - $2p_{1/2}$	$3d_{3/2}$ - 2s
	calcu-lated	experiment	ref.	calcu-lated	experiment	ref.	calcu-lated	experiment	ref.	calculated	calculated
$_{25}Mn$	1169.891	1174 1171.2±4.0	29 27	3.596			243.188			95.815	147.011
$_{26}Fe$	1254.595	1254.9±0.3 1255.4±3.0 1256.4±2.4	26 27 28	4.096			264.148	265.0±2.4	25	104.378	159.349
$_{27}Co$	1338.258	1341.5±5.0 1337±5	27 29	4.554			284.911			113.352	171.065
$_{28}Ni$	1418.98	1429.5±0.6 1429.5±5.0 1441.6±6.1	26 27 25	5.312			309.367	310.8±4.3	25	124.442	184.354
$_{29}Cu$	1510.03	1510.3±0.6 1515.1±6.0 1515	26 27 29	6.131			328.760			134.467	193.635
$_{30}Zn$	1597.29	1061.0±6.0 1590±6 1614.6±6.2	27 31 25	6.921			354.867	355.0±2.6	25	145.407	208.706
$_{31}Ga$	1686.99			7.854			375.739			156.455	218.427
$_{32}Ge$	1778.03			8.813			400.403			167.765	231.661
$_{33}As$	1872.19	1874.4±8.2 1868.3±7.0 1867±7	25 27 29	9.842			425.843	432.7±4.1	25	179.284	245.453
$_{34}Se$	1968.75			11.033			451.042			191.304	258.490

TABLE 4.2.2 - continued

Element	$2p_{3/2} - 1s$			$2p_{3/2} - 2p_{1/2}$			$3d_{5/2} - 2p_{3/2}$			$2s - 2p_{1/2}$	$3d_{3/2} - 2s$
	calculated	experiment	ref.	calculated	experiment	ref.	calculated	experiment	ref.	calculated	calculated
$_{35}Br$	2063.28			12.254			477.048			202.771	272.876
$_{37}Rb$	2244.24	2241.5±0.4	26	14.861	17.5	26	535.337			223.508	310.076
$_{38}Sr$	2340.64			16.242			569.642			234.901	334.741
$_{39}Y$	2436.70			17.683			604.728			244.912	357.649
$_{40}Zr$	2532.32	2534.0±5.1 2528.9±0.3	25 26	19.125	21.0	26	639.569	638.8±8.1	25	255.366	381.760
$_{41}Nb$	2630.21			21.267			661.175			265.707	403.817
$_{42}Mo$	2719.13	2718.5±4.6 2711.6±8.0 2711.6±8.0	25 27 32	23.564			698.447	707.5±8.1	25	270.903	428.623
$_{43}Te$	2817.70			25.628			732.510			278.472	450.826
$_{44}Ru$	2917.13			27.727			760.288			285.654	471.083
$_{45}Rh$	3011.44	2982±13	32	29.846			796.871			295.138	497.933

TABLE 4.2.2 - continued

Element	$2p_{3/2}$ - 1s			$2p_{3/2}$ - $2p_{1/2}$			$3d_{5/2}$ - $2p_{3/2}$			2s - $2p_{1/2}$	$3d_{3/2}$ - 2s
	calculated	experiment	ref.	calculated	experiment	ref.	calculated	experiment	ref.	calculated	calculated
$_{46}Pd$	3107.24	3077±10 3068	32 29	32.473			832.605			308.231	520.224
$_{47}Ag$	3205.61	3172±13 3163	32 29	35.761			865.980			316.505	544.850
$_{48}Cd$	3296.37	3258±13 3254	32 29	38.546			900.879			329.489	566.467
$_{49}In$	3392.39	3358±13 3358	32 29	40.649			939.236			339.336	594.548
$_{50}Sn$	3479.26	3457.7±0.5 3457.3±3.0 3446.4±6.4	26 28 25	43.465	45.8±0.2 44.5±1.5	26 28	977.632	982.5±3.0	28	349.526	622.196
$_{51}Sb$	3559.17	3543.3±2.0 3546 3544±15	28 29 32	45.834	48.6±1.5	28	1019.28	1019.6±3.0	28	377.605	635.400
$_{52}Te$	3648.25	3625.6±2.5	28	49.156	50.1±1.5	28	1059.54	1060.0±3.0	28	403.914	648.784
$_{53}I$	3737.28	3721.6 ±2.5	28	52.443	54.0±3.0	28	1098.74	1098.0±3.0	28	426.503	664.859
$_{55}Cs$	3905.55	3888±15	32	55.826			1188.67	1188.6±3.0	28	467.579	712.600
$_{56}Ba$	4015.25	3981±30 3985	32 29	62.461			1228.47	1229.2±3.0	28	484.423	734.905

TABLE 4.2.2 - continued

Element	$2p_{3/2} - 1s$			$2p_{3/2} - 2p_{1/2}$			$3d_{5/2} - 2p_{3/2}$			$2s - 2p_{1/2}$	$3d_{3/2} - 2s$
	calculated	experiment	ref.	calculated	experiment	ref.	calculated	experiment	ref.	calculated	calculated
$_{57}La$	4091.10	4065±15 4078	32 29	65.954			1269.43	1266.8±3.0	28	504.210	755.410
$_{58}Ce$	4190.67	4160.3±5.0	28	69.503	73.0±2.5	28	1313.11	1314.9±3.0	28	522.994	779.602
$_{59}Pr$	4291.10	4258.8±5.5	28	73.101	74.5±2.5	28	1362.42	1356.7±3.0	28	547.880	803.274
$_{60}Na$	4351.25	4335.0±6.0 4338±1	28 33	77.514	77.8±2.5	28	1408.43	1401.1±3.0	28	567.719	828.670
$_{61}Pm$	4417.18			81.426			1452.46			587.990	851.602
$_{62}Sm$	4487.38			85.219			1494.63			606.526	874.360
$_{63}Eu$	4557.68	4523±25	32	89.021			1537.15			626.642	895.871
$_{64}Gd$	4628.10			93.317			1580.65			646.772	918.164
$_{65}Tb$	4698.94			97.629			1624.78			667.032	941.153
$_{66}Dy$	4770.20			102.134			1669.90			687.421	964.854

TABLE 4.2.2 - continued

Element	$2p_{3/2} - 1s$			$2p_{3/2} - 2p_{1/2}$			$3d_{5/2} - 2p_{3/2}$			$2s - 2p_{1/2}$	$3d_{3/2} - 2s$
	calcu-lated	experiment	ref.	calcu-lated	experiment	ref.	calcu-lated	experiment	ref.	calculated	calculated
$_{67}Ho$	4841.88			106.521			1715.90			707.943	989.242
$_{68}Er$	4913.98			110.916			1762.72			728.592	1013.50
$_{69}Tm$	4986.50			115.326			1809.66			749.374	1038.98
$_{70}Yb$	5059.44			120.073			1853.29			770.280	1060.92
$_{71}Lu$	5132.80			125.219			1902.79			791.321	1087.10
$_{72}Hf$	5206.58			129.854			1952.16			812.492	1114.98
$_{73}Ta$	5280.78			134.627			2003.54			833.793	1143.85
$_{74}W$	5355.40			139.708			2055.67			855.224	1173.12
$_{75}Re$	5430.44			145.212			2108.66			876.781	1202.06
$_{76}Os$	5505.90			150.523			2162.54			898.470	1232.72

TABLE 4.2.2 - continued

Element	$2p_{3/2}$ - 1s			$2p_{3/2}$ - $2p_{1/2}$			$3d_{5/2}$ - $2p_{3/2}$			2s - $2p_{1/2}$	$3d_{3/2}$ - 2s
	calculated	experiment	ref.	calculated	experiment	ref.	calculated	experiment	ref.	calculated	calculated
$_{77}Ir$	5581.78			155.428			2216.28			920.114	1264.21
$_{78}Pt$	5658.08			161.023			2271.89			942.060	1296.21
$_{79}Au$	5734.80	5762.5±5.0 5772±9	28 34	166.584	169.7±2.0	28	2328.42	2343.1±2.5	28	964.142	1327.98
$_{80}Hg$	5811.94	5817.2±10.0 5800	28 13	172.215	172.1±2.5	28	2385.62	2388.5±4.5	28	986.35	1360.99
$_{81}Tl$	5889.72	5897.9±5.0 5930±11	28 30	179.184	181.3±2.0	28	2442.96	2446.6±2.0	28	1008.69	1395.31
$_{82}Pb$	5967.30	5966.3±5.0 5972±7 5973.98±0.44	28 34 3	185.951	185.9±2.0	28	2501.05	2499.7±1.5	28	1031.16	1427.60
$_{83}Bi$	6045.70	6030±5.5 6041±7 6053±9.0	28 34 30	189.448	192.5±3.0	28	2560.46	2554.8±2.0	28	1053.76	1462.96
$_{84}Po$	6125.32			192.217			2619.41			1074.97	1499.92
$_{85}At$	6205.64			195.589			2678.78			1096.17	1535.80
$_{87}Fa$	6316.28			204.438			2786.29			1137.57	1598.00

TABLE 4.2.2 - continued

Element	$2p_{3/2} - 1s$			$2p_{3/2} - 2p_{1/2}$			$3d_{5/2} - 2p_{3/2}$			$2s - 2p_{1/2}$	$3d_{3/2} - 2s$
	calculated	experiment	ref.	calculated	experiment	ref.	calculated	experiment	ref.	calculated	calculated
$_{88}Ra$	6377.56			207.524			2849.65			1159.37	1637.31
$_{90}Th$	6475.84			216.594			2944.33			1171.17	1704.61
$_{92}U$	6583.64			227.442			3041.13			1214.28	1750.28

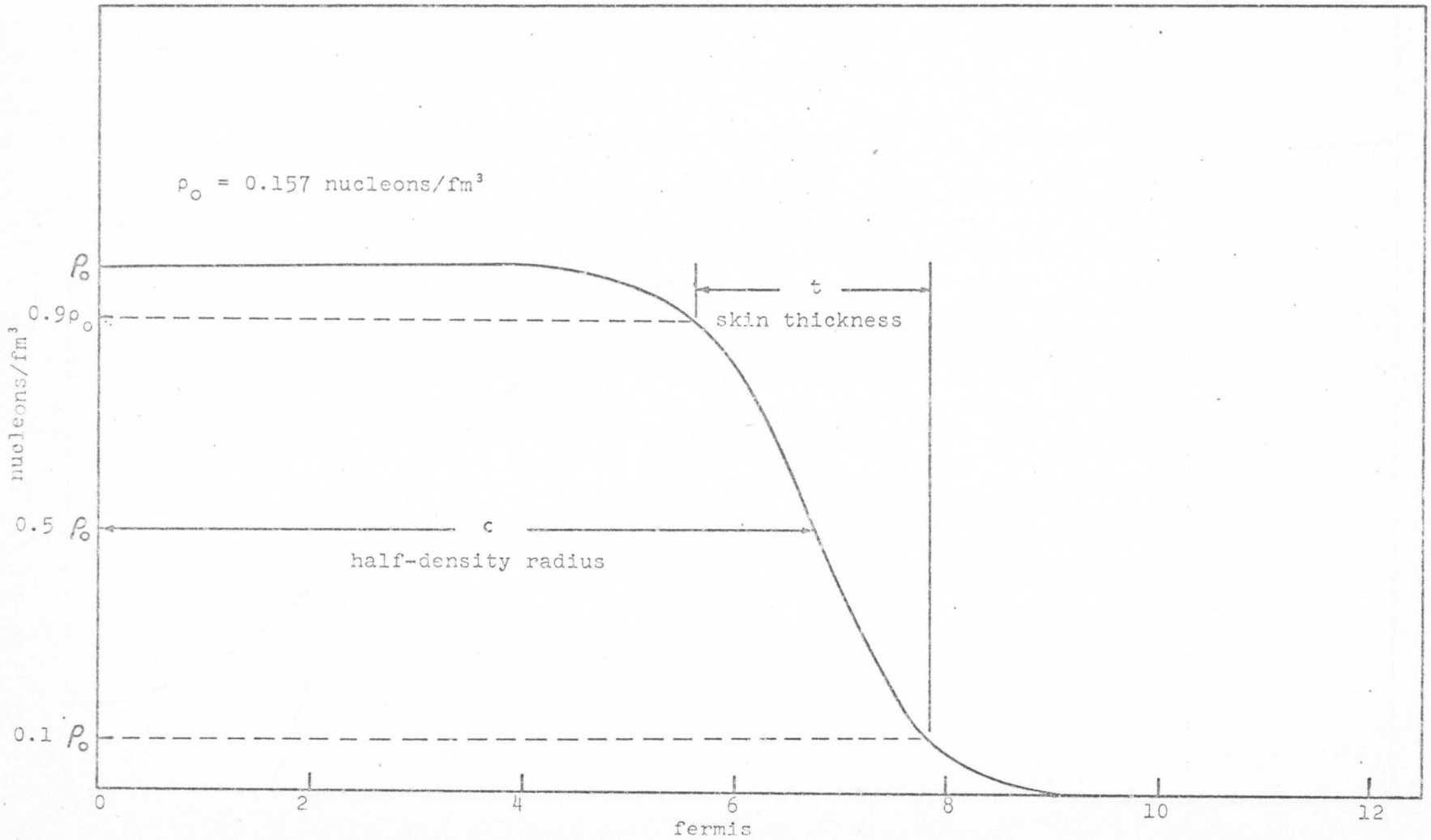

Fig. 4.2.1 The Fermi charge distribution of $_{82}Pb$ nucleus

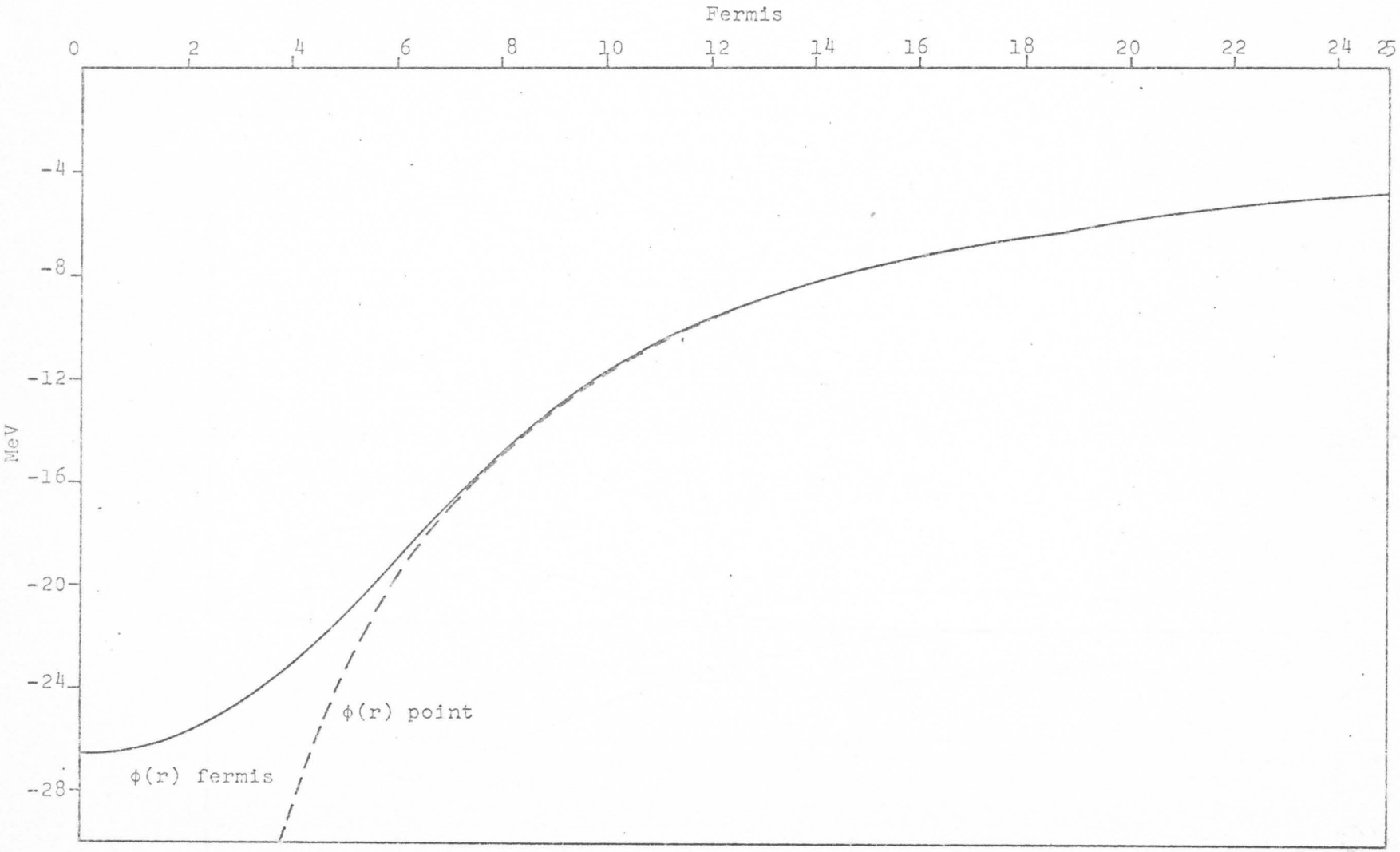

Fig. 4.2.2 Electrostatic potential energy calculated for $_{82}Pb$ using the Fermi charge distribution shown in Fig. 4.2.1 and the point nucleus charge distribution.

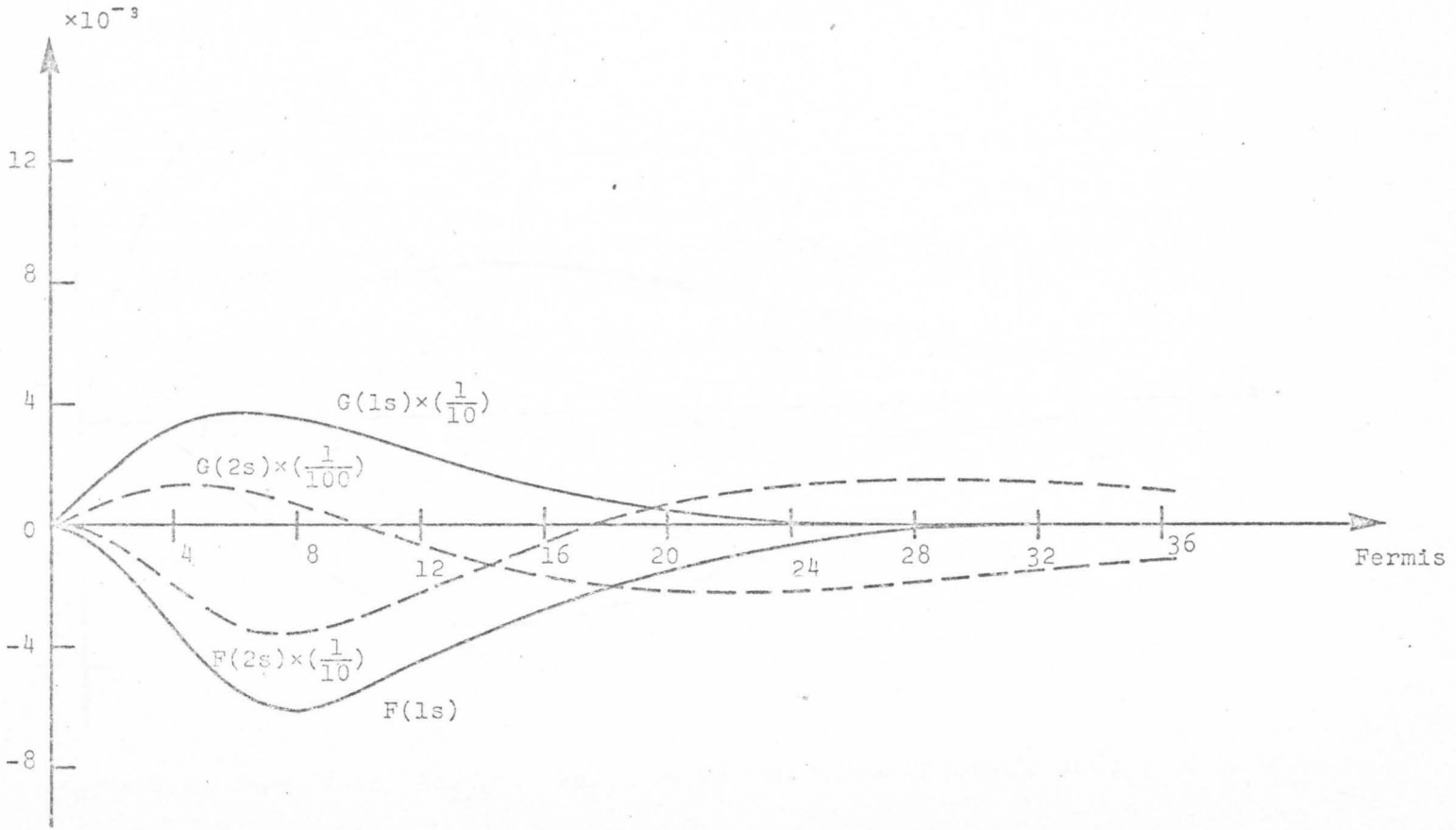

Fig. 4.2.3 Normalized 1s , 2s wave functions of muonic lead.

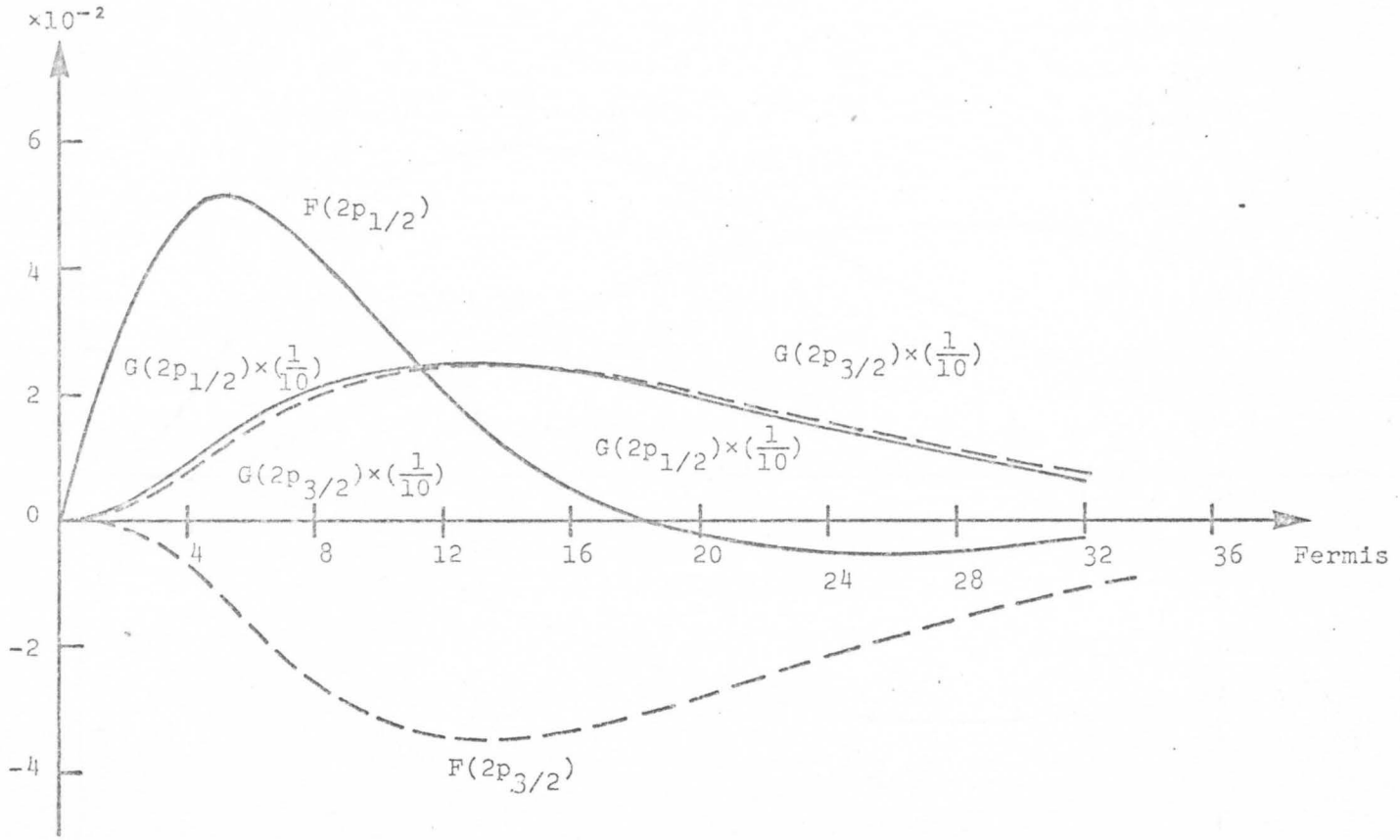

Fig. 4.2.4 Normalized $2p_{1/2}$, $2p_{3/2}$ wave functions of muonic lead.

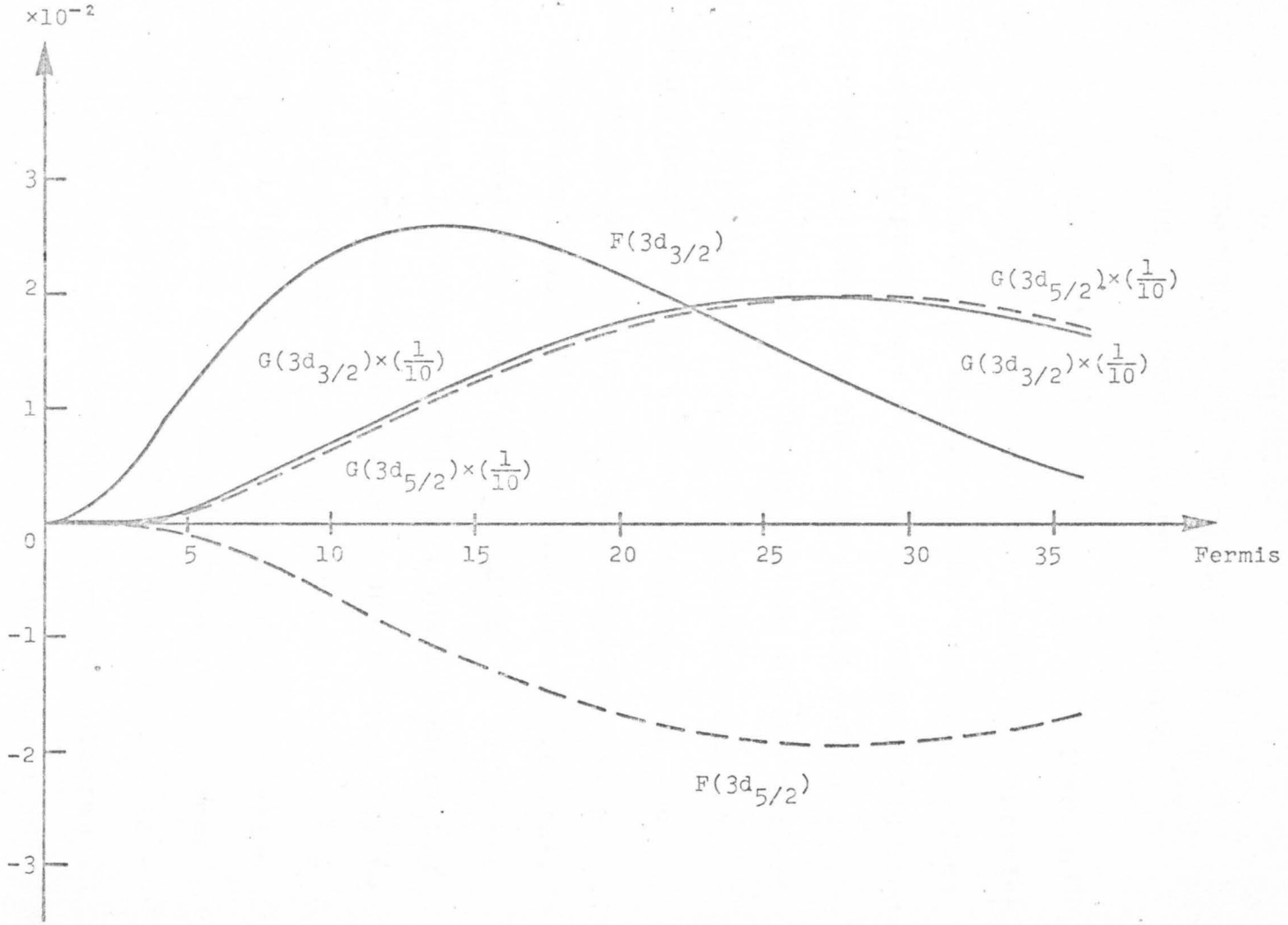

Fig. 4.2.5 Normalized $3d_{3/2}$, $3d_{5/2}$ wave functions of muonic lead.

CHAPTER 5.

EXTRACTION OF NUCLEAR PARAMETERS FROM THE MEASURED TRANSITION ENERGIES

By use of the computer program described in Chapter 4, the energy levels and the transition energies of a muonic atom can be calculated for any given values of the nuclear parameters c and t . These calculated transitions, together with the experimental values can then be used to determine the parameters of the nuclear charge distribution. Acker et al[28] represented the functional dependence of a transition energy on the parameters c and t by an iso-energetic line on a c-t diagram and made use of the fact that in general, this functional dependence on c and t is different for different transitions. That is, the iso-energetic line for one transition will usually not be parallel to the iso-energetic line for another transition, but the two lines will intersect and the point of intersection determines the value of the nuclear parameters. When the experimental error is taken into account, the iso-energetic line for a transition on the c-t diagram will become a band, and the point of intersection of two iso-energetic lines will become an area. Any c and t combination within this area is compatible with the measured energies and thus can be used to specify

the nuclear charge distribution. Usually, for the six lowest levels considered, an experiment on the muonic atom yields four independently measured energy differences[28], which can be any set of four out of six possible energy differences: $E(2p_{1/2} - 1s)$, $E(2p_{3/2} - 1s)$, $E(3d_{3/2} - 2p_{1/2})$, $E(3d_{5/2} - 2p_{3/2})$, $\Delta(2p) \equiv E(2p_{3/2}-1s) - E(2p_{1/2}-1s)$ and $\Delta(2p) - \Delta(3d) \equiv E(3d_{3/2} - 2p_{1/2}) - E(3d_{5/2} - 2p_{3/2})$. In our analysis, only two of these transitions are used in determining c and t , the remaining energy differences can be used to provide a check on the consistency of the model. If, all transitions determine a common area, the model used is consistent.

In this chapter, the method used by Acker et al[28] is closely followed to determine the parameters c and t for muonic lead. The experimental transition energies are taken from the work by Anderson et al[3].

Due to the similarity of the wave functions of the two members of a fine structure doublet, the dependence on the model and also the dependence on c and t are nearly the same for the transitions $(2p_{1/2} - 1s)$ and $(2p_{3/2} - 1s)$. The same is true for the two $3d - 2p$ transitions. Thus, the values of c and t can be determined by using one $2p - 1s$ transition and one $3d - 2p$ transition. Furthermore, it was pointed

out[34] that the $(2p_{1/2} - 1s)$ band is the narrowest and most sensitive to the parameters and that of all the other iso-energetic lines, the $(3d_{5/2} - 2p_{3/2})$ band differs most strongly in slope from the $(2p_{1/2} - 1s)$ band. Therefore, c and t are best determined by the combined values of $E(2p_{1/2} - 1s)$ and $E(3d_{5/2} - 2p_{3/2})$. These two transitions are used for the determination of the nuclear parameters for the lead nucleus.

Due to the small occupation of the 2s level of the muonic atom, the transitions involving this level are quite weak and therefore are quite difficult to measure. Up to now, only a few of these measurements have been reported. However, it was believed[3] that these transitions are quite important in the process of extracting information on the nuclear charge distribution from the experimental energies. The 2s - 2p transition has a unique sensitivity to the shape of the nuclear charge distribution. In fact, this transition is more sensitive to the skin thickness parameter t than to the half-density radius c . The corresponding iso-energetic line on a c-t diagram has a smaller slope as compared to the other lines. Thus, it will be more restrictive in the determination of c and t when this 2s - 2p transition is used in conjunction with a 2p - 1s or 3d - 2p transition. In our analysis of Pb , besides using the transitions $(2p_{1/2} - 1s)$

and $(3d_{5/2} - 2p_{3/2})$, the $(2s - 2p_{1/2})$ and the $(2p_{1/2} - 1s)$ transitions are also used to extract the nuclear parameters.

The iso-energetic line for a particular transition can be obtained in the following way: The parameter t is first fixed at a constant value and then the corresponding c is determined by means of an interpolation calculation. To do this, three different values are assigned to the parameter c. These various values of c and the constant t will form three pair of c and t combinations. For each one of these combinations, the Dirac equations are solved, using the method described in Chapter 4. In this way, the transition energies for the three c and t combinations are obtained. These calculated energies and the experimental measurements, together with a Lagrange interpolation calculation will then enable one to determine the corresponding c for this constant t. If c_1, c_2, c_3 denote the three values of the parameter c and E_1, E_2, E_3 denote the theoretically calculated energies (vacuum polarization correction included) of a particular transition (say the $(2p_{1/2} - 1s)$ transition) for c_1, c_2, c_3 respectively, then, the value of the corresponding c is given by:

$$c = c_1\frac{(E-E_2)(E-E_3)}{(E_1-E_2)(E_1-E_3)} + c_2\frac{(E-E_1)(E-E_3)}{(E_2-E_1)(E_2-E_3)} + c_3\frac{(E-E_1)(E-E_2)}{(E_3-E_1)(E_3-E_2)} \quad . \tag{5.1}$$

where E is the experimental value of the same transition. The expression (5.1) is obtained from the Lagrange interpolation formula. It can be written in a more compact form, i.e.

$$c = \sum_{i=1}^{3} c_i \prod_{\substack{k=1 \\ i \neq k}}^{3} (E-E_k)/(E_i-E_k) \quad . \tag{5.2}$$

The value of c obtained from (5.1) and the constant t determine a point on the c-t plane. Similarly, several other points on the same plane can be specified by changing the value of t to several different constants within the range of reasonable values for it, and determining their corresponding c's . A line that joins all these points is the required iso-energetic line for a particular transition. As was mentioned before, when the experimental error is taken into consideration, the corresponding c for a given t cannot be determined uniquely. As a result of this, the iso-energetic line becomes a band. The upper and lower limits of this band for a fixed t can be found by use of equation (5.2) and the experimental energy limits. If the experimental transition is given by $E_{exp} = E \pm \Delta E$, where ΔE is the error term, then the upper and lower limits of c for a given t are given by:

$$c_u = \sum_{i=1}^{3} c_i \prod_{\substack{k=1 \\ i \neq k}}^{3} [(E+\Delta E) - E_k]/[E_i - E_k] \tag{5.3}$$

and

$$c_{\ell} = \sum_{i=1}^{3} c_i \prod_{\substack{k=1 \\ i \neq k}}^{3} [(E-\Delta E) - E_k]/[E_i - E_k] \quad . \qquad (5.4)$$

For the muonic lead considered in this chapter, the fixed values for the parameter t are chosen to be 1.0 , 1.5 , 2.0 , 2.5 and 3.0 fermis while the three different assumed values of the parameter c for each fixed t are set equal to 6.0 , 6.7 and 7.4 fermis. The results of our analysis are presented in forms of tables and figures. In table 5.1 , for all three transitions considered, the values of t and their corresponding c's obtained from the interpolation calculation of equations (5.3) and (5.4) are listed. These results are also shown graphically. In figure 5.1, two iso-energetic lines (bands) corresponding to the $(2p_{1/2} - 1s)$ and the $(3d_{5/2} - 2p_{3/2})$ transitions are drawn. Due to the smallness of the experimental error, the difference between the two limiting c's (c_u and c_{ℓ}) for a fixed t in the $(2p_{1/2} - 1s)$ transition is so small that its iso-energetic band can hardly be shown on the scale used in the figure. As a result, only a heavy iso-energetic line is drawn for this transition on the c-t diagram. It can be seen from table 5.1 that the difference between the two limiting c's for a fixed t in the $(3d_{5/2}-2p_{3/2})$ transition is much larger. Thus the iso-energetic line

for this transition is a band in the diagram. This band intersects with the iso-energetic line of $(2p_{1/2} - 1s)$ and the intersection is a segment of the line (actually, the intersection of these two iso-energetics is a common area). The central point c_o , t_o and the end points c_1 , t_1 and c_2, t_2 of the intersection are indicated in the figure. Their corresponding values are given in table 5.2. The iso-energetics for the $(2p_{1/2} - 1s)$ and the $(2s - 2p_{1/2})$ transitions are shown in figure 5.2 . As explained before, the $(2p_{1/2} - 1s)$ iso-energetic band is represented by a heavy line. It can be seen from the graph that the iso-energetics of $(2s - 2p_{1/2})$ does have a smaller slope. The central and the end point values indicated in the figure are also given in table 5.2 .

The procedures for the determination of the nuclear parameters described above are quite effective for the cases of high z elements. However, its effectiveness will be greatly reduced when we deal with the low and medium z elements. One reason for this is the larger experimental error, particularly those on the 3d - 2p transitions. For these nuclei, the $3d_{5/2} - 2p_{3/2}$ transition is not accurate enough to restrict the band of values of c and t , compatible with the $2p_{1/2} - 1s$ transition. It has been shown by Acker et al[28] that if a reasonably small overlap of the two $(2p_{1/2}-1s)$ and $(3d_{5/2}-2p_{3/2})$ iso-energetic bands is to be

expected, the experimental uncertainty for the $(3d_{5/2} - 2p_{3/2})$ transition must at most be 0.1 KeV . This accuracy, unfortunately, has not yet been achieved thus far. For the low and medium z nuclei, therefore, only one parameter of the nuclear charge distribution can be derived from the measured energies. The parameter determined is usually the root mean square radius $\langle r^2 \rangle^{1/2}$ of the charge distribution or the equivalent radius to the uniform charge distribution R_{eg} , which is related to the r.m.s. radius by:

$$R_{eg}^{\ 2} = \frac{5}{3} \langle r^2 \rangle \ ; \quad \langle r^2 \rangle = \frac{\int \rho(r)\ r^2\ d\tau}{\int \rho(r)\ d\tau} \tag{5.5}$$

Backenstoss et al[24] have determined the r.m.s. radii for a group of light nuclei. Their method was to compare the experimental 2p - 1s transition with the theoretical value obtained by solving the Dirac equation for a potential produced by a Fermi-type charge distribution. The parameters c and t were varied over the whole range of reasonable values. In this way, a range of c and t combinations which are consistent with the measured energy was obtained. It was found that for all these combinations, the quantity $\langle r^2 \rangle^{1/2}$ remained practically unchanged. Thus the r.m.s. radius can be determined accurately by use of any one of these c and t combinations. Except

for the lightest nuclei, the muonic x-rays provide the most sensitive method for measuring the r.m.s. radius of the nuclear charge distribution.

Parameters / Transitions	t = 1.0		t = 1.5		t = 2.0		t = 2.5		t = 3.0	
	c_u	c_ℓ	c_u	c_ℓ	c_u	c_ℓ	c_u	c_ℓ	c_u	c_ℓ
$2p_{1/2}$-1s	6.938	6.936	6.847	6.845	6.732	6.731	6.567	6.566	6.358	6.357
$3d_{5/2}$-$2p_{3/2}$	7.052	7.041	6.935	6.924	6.763	6.752	6.516	6.505	6.254	6.243
2s-$2p_{1/2}$	6.876	6.866	6.802	6.792	6.721	6.711	6.602	6.592	6.455	6.445

TABLE 5.1 The values of c corresponding to a fixed t for the transitions of ($2p_{1/2}$-1s), ($3d_{5/2}$-$2p_{3/2}$) and (2s-$2p_{1/2}$). The units of both c and t are fm.

	Central Point		End Point			
	c_o	t_o	c_1	t_1	c_2	t_2
$(2p_{1/2}\text{-}1s)$ and $(3d_{5/2}\text{-}2p_{3/2})$	6.683	2.307	6.700	2.210	6.665	2.405
$(2p_{1/2}\text{-}1s)$ and $(2s\text{-}2p_{1/2})$	6.684	2.309	6.698	2.218	6.670	2.400

TABLE 5.2 Central and end point values of the intersections of two iso-energetic lines. The units of both c and t are fm.

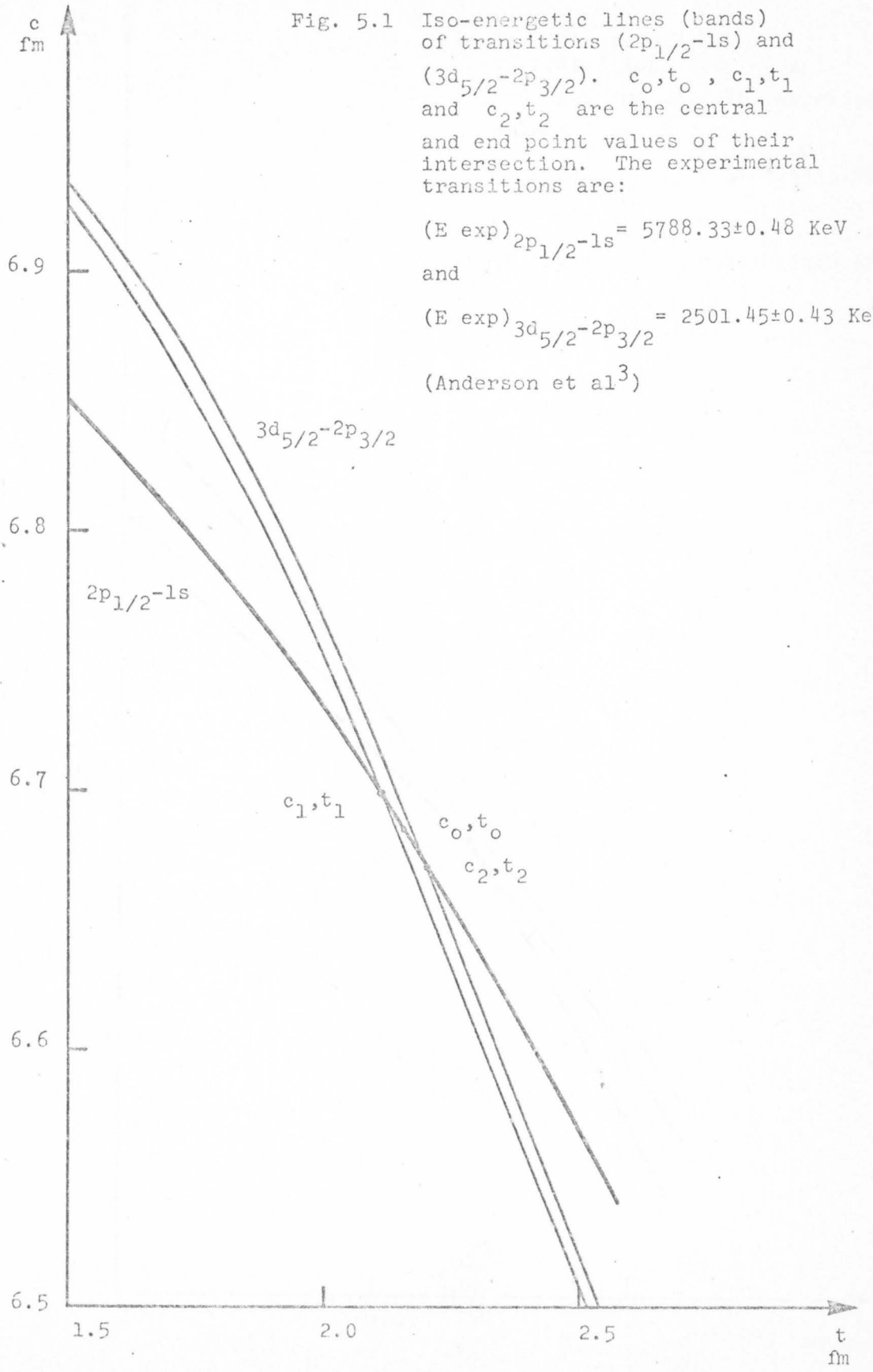

Fig. 5.1 Iso-energetic lines (bands) of transitions ($2p_{1/2}$-1s) and ($3d_{5/2}$-$2p_{3/2}$). c_o,t_o , c_1,t_1 and c_2,t_2 are the central and end point values of their intersection. The experimental transitions are:

$(E\ exp)_{2p_{1/2}-1s}$ = 5788.33±0.48 KeV

and

$(E\ exp)_{3d_{5/2}-2p_{3/2}}$ = 2501.45±0.43 KeV .

(Anderson et al[3])

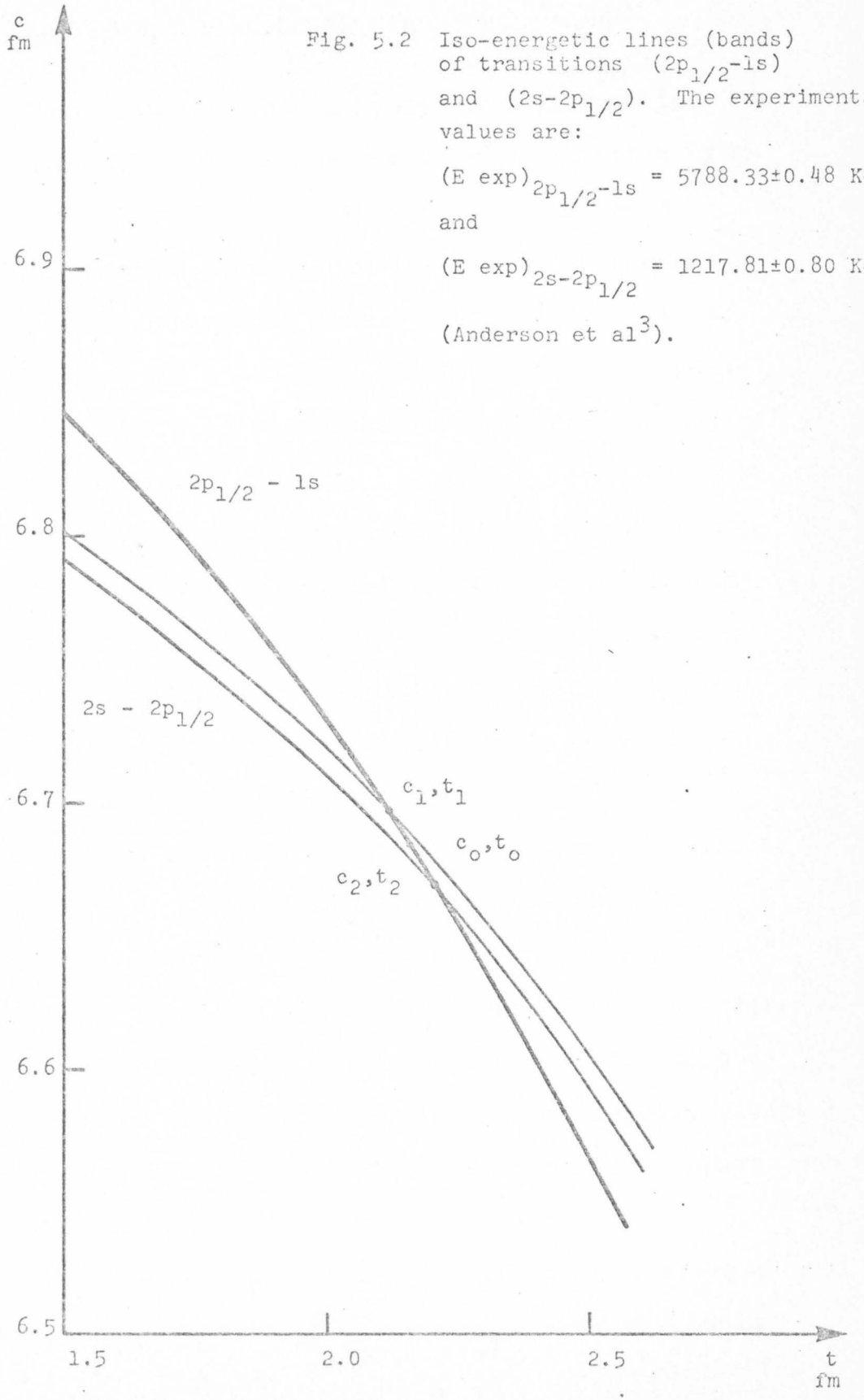

Fig. 5.2 Iso-energetic lines (bands) of transitions $(2p_{1/2}\text{-}1s)$ and $(2s\text{-}2p_{1/2})$. The experimental values are:

$(E\ exp)_{2p_{1/2}\text{-}1s} = 5788.33 \pm 0.48$ KeV

and

$(E\ exp)_{2s\text{-}2p_{1/2}} = 1217.81 \pm 0.80$ KeV .

(Anderson et al[3]).

CHAPTER 6. DISCUSSION AND CONCLUSIONS

There are two main purposes in this thesis. The first one is to calculate the binding energies of six lowest levels of muonic atoms as well as the transition energies among these levels and to compare them with the experimental data. The second one is to show how to use the calculated energies and the experimental measurements to extract information on the nuclear charge distribution.

For the first purpose, the Dirac equations are solved numerically. The Fermi-type charge distribution with parameters determined by high electron scattering experiment is used in the calculation. As can be seen from table 4.2.2, the results obtained are generally in satisfactory agreement with the experimental values. It is also found that the vacuum polarization corrections obtained for the 1s level in muonic atoms are in good agreement with the ones obtained by Ford and Wills[10]. It is believed that the small deviations of the calculated values from the experimental data are mainly due to the fact that in the calculation for the energy levels, except for the vacuum polarization, all other radiative corrections are not included.

For the second purpose, the functional dependence of a particular transition on the nuclear parameters is

represented by an iso-energetic line (band) on a c-t diagram. The values of c and t can be determined from the intersection of two different iso-energetic lines (bands). Transitions of $(2p_{1/2} - 1s)$, $(3d_{5/2} - 2p_{3/2})$ and $(2s - 2p_{1/2})$ are used in the determination of c and t for lead nucleus. It is found that the intersection of iso-energetic bands of $(2p_{1/2} - 1s)$ and $(3d_{5/2} - 2p_{3/2})$ are in fairly good agreement with the one obtained when transitions $(2p_{1/2} - 1s)$ and $(2s - 2p_{1/2})$ are used. This indicates the consistency of the model used in the analysis. It is also found that the range of c and t combinations (the intersection) obtained with the $(2p_{1/2} - 1s)$ and the $(2s - 2p_{1/2})$ transitions is somewhat smaller than the one obtained with the transitions of $(2p_{1/2} - 1s)$ and $(3d_{5/2} - 2p_{3/2})$. This result justifies the claim that is made in Chapter 5, i.e. the determination of c and t is more restrictive when a transition involving the 2s level is used.

Finally, a few words can be said about the pionic atom. It is a system consisting of a negative pion and an atomic nucleus. It has certain properties which are similar to those of the muonic atom. However, there are two main differences between them. Firstly, the pion is a spinless particle and therefore is described by the Klein-Gordon wave equation instead of the Dirac equation. Secondly, the pion interacts very strongly

with the nucleus. Thus in pionic atoms, both the electromagnetic interaction and the pion-nucleon interaction play an important role and they must be taken into account in theoretical calculations. Since pions can also be absorbed by the nucleus from the levels above the ground state, studies of pionic x-ray spectra and of the nuclear capture of negative pions in pionic atoms will provide information about the pion-nucleon interaction as well as about nuclear structure.

APPENDIX A

DERIVATION OF THE DIRAC EQUATION FOR A CENTRAL FIELD

The relativistic relation between the total energy E and the momentum $\vec{p}$ of a free particle is given by

$$E^2 = \vec{c}^2\,\vec{p}^2 + m^2c^4 \tag{A.1}$$

where m is the rest mass and c is the speed of light. Replacing E and $\vec{p}$ in eqn. (A.1) by their respective differential operators

$$E \to i\hbar\frac{\partial}{\partial t} \qquad \vec{p} \to -i\hbar\vec{\nabla} \tag{A.2}$$

where $\hbar$ is the Planck's constant and $i^2 = -1$, the Klein-Gordon equation is obtained:

$$-\hbar^2\frac{\partial^2}{\partial t^2}\Psi = -\hbar^2c^2\nabla^2\Psi + m^2c^2\Psi \tag{A.3}$$

where Ψ is the total wave function.

To find the Dirac equation for a free particle, we start from the hamiltonian form

$$i\hbar\frac{\partial}{\partial t}\Psi(\vec{r},t) = H\Psi(\vec{r},t) \tag{A.4}$$

and choose a hamiltonian which is linear in momentum and mass term. The simplest one is given by

$$H = -c\vec{\alpha}\cdot\vec{p} - \beta mc^2 \quad . \tag{A.5}$$

Here $\vec{\alpha}$, β are called the Dirac 4×4 matrices and are given by

$$\vec{\alpha} = \begin{pmatrix} 0 & \vec{\sigma} \\ \vec{\sigma} & 0 \end{pmatrix} \qquad \beta = \begin{pmatrix} 1 & 0 \\ 0 & -1 \end{pmatrix}$$

where $\vec{\sigma}$ is the Pauli spin matrix with

$$\sigma_x = \begin{pmatrix} 0 & 1 \\ 1 & 0 \end{pmatrix} \qquad \sigma_y = \begin{pmatrix} 0 & -i \\ i & 0 \end{pmatrix} \qquad \text{and} \qquad \sigma_z = \begin{pmatrix} 1 & 0 \\ 0 & -1 \end{pmatrix} .$$

By substituting (A.5) into (A.4) , we obtain the Dirac relativistic equation:

$$(E + c\vec{\alpha}\cdot\vec{p} + \beta mc^2)\Psi = 0 \quad , \tag{A.6}$$

or, using the operators (A.2)

$$(i\hbar \frac{\partial}{\partial t} - i\hbar c\vec{\alpha}\cdot\nabla + \beta mc^2)\Psi = 0 \quad . \tag{A.7}$$

Equation (A.6) or (A.7) is the Dirac relativistic equation for a free particle. If the particle is not free but subject to an external force, the Dirac equation must be modified. In the case where an electromagnetic potential is present, the modification can be made by making the replacements $c\vec{p} \rightarrow c\vec{p} - q\vec{A}(\vec{r},t)$ and $E \rightarrow E - q\phi(\vec{r},t)$, where q is the charge of the particle, $\phi(\vec{r},t)$ is the scalar potential, and $\vec{A}(\vec{r},t)$ is the vector potential. We thus obtain:

$$(E - q\phi + \vec{\alpha}\cdot(c\vec{p} - q\vec{A}) + \beta mc^2)\Psi = 0 \quad , \tag{A.8}$$

which is the Dirac equation in an external field. If the external field is central we have:

$$\vec{A}(\vec{r},t) = 0 \quad \text{and} \quad \phi(\vec{r},t) = \phi(\vec{r}) \quad . \tag{A.9}$$

By substituting (A.9) into (A.8) we obtain the Dirac equation for a central field:

$$(E - q\phi + \vec{\alpha}\cdot c\vec{p} + \beta mc^2)\Psi = 0 \tag{A.10}$$

or

$$i\hbar \frac{\partial \Psi}{\partial t} = H\Psi$$

with $H = -c\vec{\alpha}\cdot\vec{p} - \beta mc^2 + V$, and where $V = q\phi$ is the potential.

APPENDIX B MUONIC ENERGY LEVELS FOR A POINT NUCLEUS

The Dirac equations for a muon in the field of a point nucleus is given by

$$\begin{cases} \dfrac{dF(r)}{dr} = \dfrac{kF(r)}{r} - (E - \mu c^2 + \dfrac{ze^2}{r})\, G(r)/\, c \\ \dfrac{dG(r)}{dr} = -\dfrac{kG(r)}{r} + (E + \mu c^2 + \dfrac{ze^2}{r})\, F(r)/\, c \quad . \end{cases} \tag{B.1}$$

They can be solved analytically[16]. To do so, we first introduce the following notations

$$A = \frac{E + \mu c^2}{c} \tag{B.2}$$

$$B = \frac{E - \mu c^2}{c} \tag{B.3}$$

and the dimensionless length ξ, which for the case where $E \leq \mu c^2$ (i.e. bound state) is given by

$$\xi = Dr \quad , \quad D = \frac{\sqrt{\mu^2 c^4 - E^2}}{c} = \frac{\sqrt{AB}}{c} \quad . \tag{B.4}$$

Using (B.2), (B.3) and (B.4), the Dirac equation (B.1) can be transformed to a set of equations in the dimensionless variables

$$\begin{cases} (\dfrac{B}{D} + \dfrac{z\alpha}{\xi})F(\xi) - [\dfrac{d}{d\xi} + \dfrac{k}{\xi}]\, G(\xi) = 0 \\ (\dfrac{A}{D} - \dfrac{z\alpha}{\xi})\, G(\xi) - [\dfrac{d}{d\xi} - \dfrac{k}{\xi}]\, F(\xi) = 0 \quad . \end{cases} \tag{B.5}$$

We look for solutions of (B.5) in the form of a power series:

$$\begin{cases} F(\xi) = e^{-\xi} \sum_{\nu=0}^{\infty} \xi^{s+\nu} \; a_\nu & a_o \neq 0 \\ \\ G(\xi) = e^{-\xi} \sum_{\nu=0}^{\infty} \xi^{s+\nu} \; b_\nu & b_o \neq 0 \end{cases} \tag{B.6}$$

Substituting (B.6) into (B.5) and setting the coefficients of $\xi^{s+\nu-1}$ to zero we find for $\nu > 0$:

$$\begin{cases} \frac{B}{D} a_{\nu-1} + z\alpha a_\nu - (s+\nu+k)b_\nu + b_{\nu-1} = 0 \\ \\ \frac{A}{D} b_{\nu-1} - z\alpha b_\nu - (s+\nu-k)a_\nu + a_{\nu-1} = 0 \quad . \end{cases} \tag{B.7}$$

When $\nu = 0$, equation (B.7) reduces to

$$\begin{cases} z\alpha a_o - (s+k)b_o = 0 \\ \\ -(s-k)a_o - z\alpha b_o = 0 \quad . \end{cases} \tag{B.8}$$

Equations (B.8) have the required nonvanishing solution for a_o and b_o if and only if the determinant of their coefficients is equal to zero, i.e. if

$$\begin{vmatrix} z\alpha & -(s-k) \\ -(s+k) & -z\alpha \end{vmatrix} = 0 \quad .$$

From this we have

$$(z\alpha)^2 + s^2 - k^2 = 0$$

or $$s = \pm \sqrt{k^2 - (z\alpha)^2} \quad . \tag{B.9}$$

We only take the positive sign for s in (B.9) and drop the solution corresponding to the negative sign in front of (B.9) as it leads to a wavefunction diverging at the origin, and thus violates the boundary condition there.

Multiplying the first equation in (B.7) by D and the second by B, subtracting the one from the other and using (B.4), we find a relation between the coefficients a_ν and b_ν :

$$a_\nu[\sqrt{\frac{A}{B}}\, z\alpha + s + \nu - k\,] = b_\nu[\sqrt{\frac{A}{B}}\,(s + \nu + k) - z\alpha\,] \,. \tag{B.10}$$

The series (B.6) will correspond to solutions which are well-behaved at infinity, if they terminate for a finite value $\nu = N$. Putting $a_{N+1} = b_{N+1} = 0$ in (B.7), we find

$$\sqrt{B}\, a_N = -\sqrt{A}\, b_N \,, \quad N = 0, 1, 2, \ldots . \tag{B.11}$$

Substituting (B.11) into (B.10) and putting $\nu = N$, we obtain the following equation

$$\frac{B-A}{D}\, z\alpha = z(s+N) \quad . \tag{B.12}$$

Substituting (B.2), (B.3) and (B.4) into (B.12)

we get

$$z\alpha E = -(s+N)\sqrt{\mu^2c^4 - E^2} \quad . \tag{B.13}$$

Replacing s by the expression (B.9) and squaring (B.13), we have

$$(z\alpha)^2E^2 = [(\sqrt{k^2-(z\alpha)^2}) + N]^2(\mu c^2 - E^2) \quad . \tag{B.14}$$

From this equation, the total energy E can easily be found:

$$E = \mu c^2\left[1 + \left(\frac{z\alpha}{N+\sqrt{k^2-z^2\alpha^2}}\right)^2\right]^{-1/2} \quad , \tag{B.15}$$

with $k = \pm 1, \pm 2, \ldots$ $\qquad N = 0, 1, 2, \ldots$.

For $N = 0$, k can only take a negative value. The principle quantum number n is related to N by the relation

$$n = N + |k| \quad . \tag{B.16}$$

In terms of n , the total energy E can be written as:

$$E = \mu c^2\left[1 + \left(\frac{z\alpha}{n-|k| +\sqrt{k^2-z^2\alpha^2}}\right)^2\right]^{-1/2} \quad . \tag{B.17}$$

The binding energies E_b of various levels are given by

$$E_b = \mu c^2 - E = \mu c^2\left\{1 - \left[1 + \left(\frac{z\alpha}{N+\sqrt{k^2-z^2\alpha^2}}\right)^2\right]^{-1/2}\right\} \quad . \tag{B.18}$$

APPENDIX C

MATHEMATICAL FORMULAE USED IN THE NUMERICAL INTEGRATION

I. Simpson's Rule:

Let I denote the definite integral which is given by

$$I = \int_{a}^{a+2h} f(x)\,dx \quad , \tag{C.1}$$

then the numerical approximation of this integral is given by

$$I = \frac{[(a+2h)-a]}{6}\,[f(a) + 4f(a+h) + f(a+2h)]$$

$$= \frac{h}{3}\,[f(a) + 4f(a+h) + f(a+2h)] \quad . \tag{C.2}$$

This is known as Simpson's rule.

II. Fourth-order Runge-Kutta Method for a System of Two First-order Equations:

In the following, the formulae for the fourth-order Runge-Kutta method are stated, their detailed derivation can be found in some numerical analysis texts.[44]

If
$$\begin{aligned} y_1' &= f_1(x, y_1, y_2) \qquad & y_1(x_o) &= y_{10} \\ y_2' &= f_2(x, y_1, y_2) \qquad & y_2(x_o) &= y_{20} \end{aligned} \tag{C.3}$$

denote a system of two first-order equations and their initial conditions, then, using the notation $x_i = x_o + ih$, $i = 1, 2, 3, \ldots$, and $y_{1,i}$, $y_{2,i}$ as the numerical approximations to $y_1(x_i)$, $y_2(x_i)$, we have:

$$\begin{aligned} y_{1,i+1} &= y_{1,i} + h\,\phi_1(x_i, y_{1,i}, y_{2,i}; h) \\ y_{2,i+1} &= y_{2,i} + h\,\phi_2(x_i, y_{1,i}, y_{2,i}; h) \end{aligned} \qquad (C.4)$$

where

$$\begin{aligned} \phi_1(x_i, y_{1,i}, y_{2,i}; h) &= \frac{1}{6}\,(k_{11} + 2k_{12} + 2k_{13} + k_{14}) \\ \phi_2(x_i, y_{1,i}, y_{2,i}; h) &= \frac{1}{6}\,(k_{21} + 2k_{22} + 2k_{23} + k_{24}) \end{aligned} \qquad (C.5)$$

and

$$\begin{aligned} k_{11} &= f_1(x_i, y_{1,i}, y_{2,i}) \\ k_{21} &= f_2(x_i, y_{1,i}, y_{2,i}) \\ k_{12} &= f_1\left(x_i + \frac{h}{2}\,,\ y_{1,i} + \frac{h}{2}\,k_{11}\,,\ y_{2,i} + \frac{h}{2}\,k_{21}\right) \\ k_{22} &= f_2\left(x_i + \frac{h}{2}\,,\ y_{1,i} + \frac{h}{2}\,k_{11},\ y_{2,i} + \frac{h}{2}\,k_{21}\right) \\ k_{13} &= f_1\left(x_i + \frac{h}{2}\,,\ y_{1,i} + \frac{h}{2}\,k_{12},\ y_{2,i} + \frac{h}{2}\,k_{22}\right) \\ k_{23} &= f_2\left(x_i + \frac{h}{2},\ y_{1,i} + \frac{h}{2}\,k_{12},\ y_{2,i} + \frac{h}{2}\,k_{22}\right) \\ k_{14} &= f_1(x_i + h,\ y_{1,i} + hk_{13},\ y_{2,i} + hk_{23}) \\ k_{24} &= f_2(x_i + h,\ y_{1,i} + hk_{13},\ y_{2,i} + hk_{23}) \end{aligned} \qquad (C.6)$$

.

APPENDIX D COMPUTER PROGRAM WRITTEN TO CALCULATE THE ENERGY LEVELS OF MUONIC ATOMS

```
C
C       FORTRAN PROGRAM FOR THE CALCULATION OF ENERGY LEVELS AND THEIR
C       CORRESPONDING VACUUM POLARIZATION CORRECTIONS OF MUONIC ATOMS
C
        IMPLICIT REAL *8 (A-H,O-Z)
        DOUBLE PRECISION LM,LA
        DIMENSION Y(2),R(2,4),YB(2),YBI(2),YA(2),YAB(2),YABI(2),XX(501),
       1V(1001),EE(3),DD(3),VP(501),VL(501),SY(2,501),YY(2,501)
        COMMON K
C
C       F(X,XP,FN,FC) AND FVL(X,XP,C,LA,FN,FC) ARE THE INTEGRANDS IN
C       EONS. (2.2.6A) AND (3.1.7)
C
        F(X,XP,FN,FC)=(XP**2-X*XP)/(1.0+DEXP(FN*(XP/FC-1.0)))
        FVL(X,XP,C,LA,FN,FC)=XP*(DABS(X-XP)*(DLOG(C*DABS(X-XP)/LA)-1.0)
       1-(X+XP)*(DLOG(C*(X+XP)/LA)-1.0))/(1.0+DEXP(FN*(XP/FC-1.0)))
C
C       READ IN THE CONSTANTS. ALL LENGTHS ARE IN FERMIS. Z IS THE
C       ATOMIC NO., LM AND LA ARE THE REDUCED COMPTON WAVELENGTH OF THE
C       MUON AND ELECTRON, FN AND FC ARE THE NUCLEAR PARAMETERS 'C' AND
C       'N', C IS THE CONSTANT IN (3.1.7), O IS THE ELECTRONIC CHARGE,
C       H IS THE STEP SIZE OF THE INTEGRATION, XX(1) IS THE STARTING POINT
C       OF THE INTEGRATION, UP IS THE UPPER LIMIT OF THE INTEGRAL
C       IN (2.2.6A), AP IS THE FINE STRUCTURE CONSTANT AND EB IS THE
C       ELECTROSTATIC POTENTIAL FOR THE POINT NUCLEUS AT THE STARTING
C       POINT. Z, LM, FN AND FC ARE DIFFERENT FOR DIFFERENT ATOM. THE
C       REST ARE THE SAME FOR ALL ATOMS.
C
        Z=82.0
        LM=1.867525961
        FC=6.391
        FN=11.716
        LA=0.3861503
        C=1.781
        O=4.80286D-10
        H=0.25
        XX(1)=0.1D-2
        VX=XX(1)
        PI=3.1416
        H2=H/2.0
        UP=30.0
        EB=1.0D3
        AP=0.7299270-2
        DO 60 I=1,350
   60   XX(I+1)=XX(I)+H
        DO 1 K=1,801
C
C       CALCULATION OF THE ELECTROSTATIC POTENTIAL GIVEN BY (2.2.6A)
C       BY SIMPSON'S RULE.
C
        X1=VX
C
C       VX REFERS TO THE VARIABLE 'R' AND X1,X2,XM REFER TO VARIABLE (R')
C
        SUM=0.0
        IF(X1.GE.UP) GO TO 22
   21   X2=X1+H
        XM=(X1+X2)/2.0
```

```
      DUMMY=F(VX,X1,FN,FC)+4.0*F(VX,XM,FN,FC)+F(VX,X2,FN,FC)
      SUM=SUM+DUMMY
      X1=X2
      IF(X2.LT.UP) GO TO 21
      SUM=SUM*H/6.0
C
C     SUM IS THE VALUE OF THE INTEGRAL IN (2.2.6A)
C
   22 V(K)=  1./VX-3.*SUM/((FC**3*VX)*(1.0+PI**2/FN**2))
C
C     V(K) IS THE VALUE OF THE ELECTROSTATIC POTENTIAL AT THE POINT
C     R=VX
C
      VX=VX+H2
    1 CONTINUE
C
C     CALCULATION OF THE EFFECTIVE POTENTIAL DUE TO VACUUM POLARIZATION
C
      DO 10 I=1,349
      X1=0.0
      SUM1=0.0
C
C     CALCULATION OF THE INTEGRATION W. R. T. R' IN (3.1.7) BY SIMPSON'S R
C
      DO 12 J=1,120
      X2=X1+H
      DUM=(X1+X2)/2.0
      DUMMY=FVL(XX(I),X1,C,LA,FN,FC)+4.0*FVL(XX(I),DUM,C,LA,FN,FC)
     1+FVL(XX(I),X2,C,LA,FN,FC)
      X1=X2
   12 SUM1=SUM1+DUMMY
      SUM1=SUM1*H/6.0
C
C     SUM1 IS THE RESULT OF THE INTEGRATION IN (3.1.7)
C
      VL(I)=-3.0*SUM1/(2.0*XX(I)*FC**3*(1.0+PI**2/FN**2))
      II=2*I-1
      VP(I)=2.0*AP*(VL(I)+5.0*V(II)/6.0)/(3.0*PI)
C
C     VP(I) IS THE VACUUM POLARIZATION POTENTIAL AT R=XX(I)
C
   10 CONTINUE
C
C     START TO SOLVE THE DIRAC EQNS. THE NO. '6' IN THE "DO LOOP"
C     INDICATES THE CALCULATION IS REPEATED 6 TIMES FOR 6 LOWEST LEVELS
C     CONSIDERED
C
      DO 311 IK=1,6
C
C     READ IN CONSTANTS WHICH ARE DIFFERENT FOR DIFFERENT LEVEL.
C     "K" IS THE QUANTUM NO. K IN THE DIRAC EQNS. "EA" IS THE DIMENSIONLES
C     ENERGY FOR THE POINT NUCLEUS,"DE" IS THE 'DELTA EPSILON' IN
C     EQN.(4.1.10),AND RA IS THE VALUE OF THE MATCHING RADIUS.ALL FOUR
C     OF THESE CONSTANTS FOR A PARTICULAR LEVEL ARE PUNCHED IN CERTAIN
C     COLUMNS IN THE SAME DATA CARD SPECIFIED BY THE FORMAT."K" IS AN
C     INTEGER AND IS PUNCHED IN COLUMNS 1 TO 3 WITH THE LAST FIGURE IN
C     COLUMN 3."EA" IS A REAL NO. OF TEN DIGITS AND IS PUNCHED IN
C     COLUMNS 4 TO 18 WITH THE LAST FIGURE IN COLUMN 18."DE" IS A REAL
```

```
C       NO. EXPRESSED IN EXPONENTIAL FORM AND IS PUNCHED IN COLUMNS
C       19 TO 30 WITH THE LAST FIGURE IN COLUMN 30."RA" IS A REAL NO.
C       AND IS PUNCHED IN COLUMNS 31 TO 35 WITH THE LAST FIGURE IN COLUMN 3
C
        READ(5,310)K,EA,DE,RA
  310   FORMAT(I3,F15.10,D12.3,F5.1)
        PRINT 41,K
   41   FORMAT('1',*K=',I3)
        XA=XX(1)
C
C       XA IS THE VARIABLE "R" IN THE DIRAC EQNS. FOR THE POINT NUCLEUS
C       CASE
C
        IF(K.GT.0.0) GO TO 40
C
C       THE TEST STATEMENT CHOOSES THE APPROPRIATE ASYMPTOTIC SOLUTIONS
C       FOR THE LEVEL BEING CONSIDERED.YA(1),YA(2) ARE THE INITIAL VALUES
C       OF THE POINT NUCLEUS RADIAL WAVE FUNCTIONS "F" AND"G" WHICH ARE
C       GIVEN BY EQNS.(4.1.7) OR (4.1.8)
C
        YA(1)=-(AP*Z*EB+(EA-1.0)/LM)*XA**(-K+1)/(-2*K+1)
        YA(2)=XA**(-K)
        GO TO 54
   40   YA(1)=(2*K+1)*XA**K/((EA+1.0)/LM+AP*Z*EB)
        YA(2)=XA**(K+1)
C
C       SOLUTION OF THE POINT NUCLEUS DIRAC EQNS. BY 4TH ORDER RUNGE-KUTTA
C       METHOD.GP(I,.....EA) ARE THE FUNCTIONS GIVEN BY EQN.(2.3.2) AND
C       APPEAR IN THE FUNCTIONAL SUBPROGRAM GP(I,XA,YA,EA)
C
   54   DO 45 I=1,2
        R(I,1)=GP(I,XA,YA,EA)
C
C       R(I,1) ARE THE QUANTITIES K11,K21 IN EQN.(4.1.6)
C
   45   YAB(I)=YA(I)+H2*R(I,1)
C
C       YAB(I) ARE THE QUANTITIES YI,1+(H/2)K11 AND YI,2+(H/2)K21 IN
C       EQN.(4.1.6)
C
        XAB=XA+H2
        XA=XA+H
        DO 46 I=1,2
        R(I,2)=GP(I,XAB,YAB,EA)
C
C       R(1,2) ARE THE QUANTITIES K21,K22 IN EQN.(4.1.6)
C
   46   YAB1(I)=YA(I)+H2*R(I,2)
C
C       YAB1(I) ARE THE QUANTITIES YI,1+(H/2)K21 AND YI,2+(H/2)K22 IN
C       EQN.(4.1.6)
C
        DO 47 I=1,2
        R(I,3)=GP(I,XAB,YAB1,EA)
C
C       R(I,3) ARE THE QUANTITIES K31,K32 IN EQN.(4.1.6)
C
   47   YAB(I)=YA(I)+H*R(I,3)
```

```
C
C       YAB(I) ARE THE QUANTITIES YI,1+(H)K31,YI,2+(H)K32 IN EQN.(4.1.6)
C
        DO 48 I=1,2
   48   R(I,4)=GP(I,XA,YAB,EA)
C
C       R(I,4) ARE THE QUANTITIES K41,K42 IN EQN.(4.1.6)
C
        DO 49 I=1,2
   49   YA(I)=YA(I)+ (H/6.0)*(R(I,1)+2.0*(R(I,2)+R(I,3))+R(I,4))
C
C       YA(I) ARE THE SOLUTIONS OF YA AT R=(XA+H)(THE SOLUTIONS GIVEN BY
C       EQN.(4.1.4))
C
        IF(XA.GE.RA) GO TO 53
C
C       THE TEST STATEMENT INDICATES THAT WHEN R REACHES THE MATCHING
C       RADIUS,THE CALCULATION FOR THE POINT NUCLEUS IS STOPPED. THE
C       VALUES OF WAVE FUNCTIONS "F"AND"G"AT THE MATCHING RADIUS ARE STORED
C       UP FOR LATER USE. THE PROGRAM IS THEN MOVED TO THE SOLUTION OF
C       THE DIRAC EQNS. FOR A FINITE NUCLEUS.
C
        GO TO 54
   53   ES=EA
C
C       "ES" IS THE DIMENSIONLESS ENERGY'EPSILON' IN THE FINITE NUCLEUS CASE
C
        IN=0
  300   ES0=ES
C
C       "ES0" DENOTES THE PREVIOUS EIGENVALUE OBTAINED IN THE INTERPOLATION
C       CALCULATION
C
   11   IN=IN+1
C
C       "IN" INDICATES THE NO. OF TIMES THAT THE FINITE NUCLEUS DIRAC EQNS.
C       ARE SOLVED.
C
        IF(IN.GT.3) GO TO 51
C
C       AFTER THE FINITE NUCLEUS DIRAC EQNS. ARE SOLVED 3 TIMES WITH 3
C       DIFFERENT EIGENVALUES,THE PROGRAM IS THEN MOVED TO THE INTERPOLATION
C       CALCULATION.
C
        EE(IN)=ES
C
C       "EE(IN)" ARE THE QUANTITIES 'EPSILON1','EPSILON2' AND 'EPSILON3'
C       IN EQNS.(4.1.11) AND (4.1.12)
C
        E=V(1)
C
C       "E" IS THE ELECTROSTATIC POTENTIAL OF A FINITE NUCLEUS AT THE
C       STARTING POINT R=0.001 FM.
C
C       SOLUTION OF THE FINITE NUCLEUS DIRAC EQNS. BY 4TH ORDER RUNGE-KUTTA
C       METHOD. EXPANATIONS OF THE QUANTITIES ARE SIMILAR TO THOSE GIVEN
C       ABOVE FOR THE POINT NUCLEUS.
C
```

```
      X=XX(1)
      IF(K.GT.0.0) GO TO 42
      Y(1)=-(AP*Z*E+(ES-1.0)/LM)*X**(-K+1)/(-2*K+1)
      Y(2)=X**(-K)
      GO TO 43
   42 Y(1)=(2*K+1)*X**K/((ES+1.0)/LM+AP*Z*E)
      Y(2)=X**(K+1)
   43 ID=1
    2 IV=2*ID-1
      ID=ID+1
      DO5 I=1,2
      R(I,1)=G(I,X,Y,ES,V(IV))
    5 YB(I)=Y(I)+H2*R(I,1)
      XB=X+H2
      X=X+H
      DO 6 I=1,2
      R(I,2)=G(I,XB,YB,ES,V(IV+1))
    6 YB1(I)=Y(I)+H2*R(I,2)
      DO7 I=1,2
      R(I,3)=G(I,XB,YB1,ES,V(IV+1))
    7 YB(I)=Y(I)+H*R(I,3)
      DO8 I=1,2
    8 R(I,4)=G(I,X,YB,ES,V(IV+2))
      DO9 I=1,2
    9 Y(I)=Y(I)+(H/6.0)*(R(I,1)+2.0*(R(I,2)+R(I,3))+R(I,4))
      IF(X.GE.RA) GO TO 50
C
C     WHEN "R" REACHES THE MATCHING RADIUS,THE INTEGRATION IS STOPPED
C     AND THE PROGRAM IS MOVED TO CALCULATE THE DIFFERENCE "D" GIVEN BY
C     EQN.(4.1.9)
C
      GO TO 2
   50 DD(IN)=Y(1)*YA(2)-Y(2)*YA(1)
C
C     "DD(IN)" DENOTES THE QUANTITY GIVEN BY EQN.(4.1.9)
      ES=ES+DE
C
C     "ES" DENOTES THE NEW TRIAL EIGENVALUE.
C
      GO TO 11
   51 E12=(-DD(1)*EE(2)+DD(2)*EE(1))/(DD(2)-DD(1))
      E13=(-DD(1)*EE(3)+DD(3)*EE(1))/(DD(3)-DD(1))
      E123=(-DD(2)*E13+DD(3)*E12)/(DD(3)-DD(2))
C
C     INTERPOLATION CALCULATION GIVEN BY EQNS.(4.1.11) TO (4.1.13)
C
      DDE=DABS(E123-ES0)
      IF(DDE.LE.1.0D-8) GO TO 52
C
C     EXAMINE THE DIFFERENCE BETWEEN TWO SUCCESSIVE TRIAL EIGENVALUES.
C
      ES=E123
C
C     "ES" IS THE NEW TRIAL EIGENVALUE.
C
      DE=0.2*DE
C
C     "DE" IS THE NEW INCREAMENT OF "ES".
```

```
C
      IN=0
      GO TO 300
   52 ES=E123
C
C     "ES" IS THE CORRECT EIGENVALUE FOR FINITE NUCLEUS DIRAC EQNS.
C
      PRINT 101,ES
  101 FORMAT('-','EXACT ES=',D20.10)
      RA=207.2
C
C     "RA" IS THE MASS NO. OF THE ATOM.
C
      RM=105.69*RA/(RA+0.1135)  MeV
C
C     "RM" IS THE REDUCED MASS OF THE MUON GIVEN BY EQN.(4.1.16)
C
      BE=-RM*(1.0-ES)*1.0D3  keV
C
C     "BE" IS THE BINDING ENERGY OF THE LEVEL CONSIDERED.
C
      PRINT 102,BE
  102 FORMAT('-','BE(KEV)=',D20.10)
C
C     CALCULATION OF THE FINITE NUCLEUS RADIAL WAVE FUNCTIONS "F" AND
C     "G" BY 4TH ORDER RUNGE-KUTTA METHOD.
C
      X=XX(1)
      IF(K.GT.0.0) GO TO 33
      Y(1)=-(AP*Z*E+(ES-1.0)/LM)*X**(-K+1)/(-2*K+1)
      Y(2)=X**(-K)
      GO TO 34
   33 Y(1)=(2*K+1)*X**K/((ES+1.0)/LM+AP*Z*E)
      Y(2)=X**(K+1)
   34 ID=1
      SY(1,1)=Y(1)
      SY(2,1)=Y(2)
   32 IV=2*ID-1
      ID=ID+1
C
C     "ID","IV" ARE INDICES.
C
      IF(ID.EQ.200) GO TO 16
C
C     IF R=50 FERMIS,THE INTEGRATION IS STOPPED.THE PROGRAM IS THEN
C     MOVED TO THE CALCULATION OF THE VACUUM POLARIZATION CORRECTION.
C
      DO 35 I=1,2
      R(I,1)=G(I,X,Y,ES,V(IV))
   35 YB(I)=Y(I)+H2*R(I,1)
      XB=X+H2
      X=X+H
      DO 36 I=1,2
      R(I,2)=G(I,XB,YB,ES,V(IV+1))
   36 YB1(I)=Y(I)+H2*R(I,2)
      DO 37 I=1,2
      R(I,3)=G(I,XB,YB1,ES,V(IV+1))
   37 YB(I)=Y(I)+H*R(I,3)
```

```
      DO 38 I=1,2
   38 R(I,4)=G(I,X,YB,ES,V(IV+2))
      DO 39 I=1,2
      Y(I)=Y(I)+(H/6.0)*(R(I,1)+2.0*(R(I,2)+R(I,3))+R(I,4))
   39 SY(I,ID)=Y(I)
C
C     ALL VALUES OF "F" AND "G" OBTAINED FOR DIFFERENT R ARE STORED UP.
C
      GO TO 32
C
C     NORMALIZATION OF THE WAVE FUNCTIONS "F" AND "G". SIMPSON'S RULE
C     IS USED.
C
   16 ID=ID-3
C
C     CALCULATION OF THE NORMALIZATION CONSTANT GIVEN BY EQN.(4.1.19)
C
      AA=0.0
      DO 13 I=1,ID,2
      I1=I+1
      I2=I+2
C
C     "I1","I2" ARE INDICES.
C
      DUMMY=(SY(1,I)**2+SY(2,I)**2)+4.0*(SY(1,I1)**2+SY(2,I1)**2)
     1+(SY(1,I2)**2+SY(2,I2)**2)
   13 AA=AA+DUMMY
      AA=AA*H/3.0
C
C     "AA" IS THE SQUARE OF THE NORMALIZATION CONSTANT (N**2) GIVEN BY
C     EQN.(4.1.19)
C
      PRINT17,AA
   17 FORMAT('-','AA=',D20.10)
      DO 44 J=1,199
      YY(1,J)=SY(1,J)/DSQRT(AA)
      YY(2,J)=SY(2,J)/DSQRT(AA)
   44 CONTINUE
C
C     CALCULATION OF THE VACUUM POLARIZATION CORRECTION. SIMPSON'S RULE
C     IS USED.
C
      EP=0.0
      DO 14 I=1,ID,2
      I1=I+1
      I2=I+2
C
C     EVALUATION OF THE INTEGRAL IN EQN.(3.1.9)
C
      DUMMY=(YY(1,I)**2+YY(2,I)**2)*VP(I)+4.0*(YY(1,I1) **2+YY(2,
     1I1) **2)*VP(I1) +(YY(1,I2) **2+YY(2,I2) **2)*VP(I2)
   14 EP=EP+DUMMY
      EP=EP*H/3.0
      EP=EP*Z*0**2/1.60206D-22
C
C     "EP" DENOTES THE ENERGY SHIFT DUE TO VACUUM POLARIZATION IN 'KEV'
C
      PRINT 15,EP
```

```
 15 FORMAT('-','EP(KEV)=',D20.10)
311 CONTINUE
    CALL EXIT
    END
```

```
      FUNCTION GP(I,XA,YA,EA)
C
C     FUNCTIONAL SUBPROGRAM FOR THE POINT NUCLEUS DIRAC EQNS.
C     GP(I,XA,YA,EA) ARE THE EXPRESSIONS ON THE RIGHT-HAND SIDE OF THE
C     POINT NUCLEUS DIRAC EQNS. GIVEN BY EQNS.(2.3.2)
C
      IMPLICIT REAL *8 (A-H,O-Z)
      DOUBLE PRECISION LM
      DIMENSION YA(2)
      COMMON K
      Z=82.0
      LM=1.867825961
      AP=0.729927E-2
      GO TO(1,2),I
    1 GP=K*YA(1)/XA-((EA-1.0)/LM+Z*AP/XA)*YA(2)
      RETURN
    2 GP=-K*YA(2)/XA+((EA+1.0)/LM+Z*AP/XA)*YA(1)
      RETURN
      END
```

```
      FUNCTION GP(I,XA,YA,EA)
C
C     FUNCTIONAL SUBPROGRAM FOR THE POINT NUCLEUS DIRAC EQNS.
C     GP(I,XA,YA,EA) ARE THE EXPRESSIONS ON THE RIGHT-HAND SIDE OF TH
C     POINT NUCLEUS DIRAC EQNS. GIVEN BY EQNS.(2.3.2)
C
      IMPLICIT REAL *8 (A-H,O-Z)
      DOUBLE PRECISION LM
      DIMENSION YA(2)
      COMMON K
      Z=82.0
      LM=1.867825961
      AP=0.729927E-2
      GO TO(1,2),I
    1 GP=K*YA(1)/XA-((EA-1.0)/LM+Z*AP/XA)*YA(2)
      RETURN
    2 GP=-K*YA(2)/XA+((EA+1.0)/LM+Z*AP/XA)*YA(1)
      RETURN
      END
```

```
      FUNCTION G(I,X,Y,ES,V)
C
C     FUNCTIONAL SUBPROGRAM FOR THE FINITE NUCLEUS DIRAC EQNS.
C     G(I,X,Y,ES,V) ARE THE EXPRESSIONS ON THE RIGHT-HAND SIDE OF THE
C     FINITE NUCLEUS DIRAC EQNS. GIVEN BY EQNS.(2.2.9)
C
      IMPLICIT REAL *8 (A-H,O-Z)
      DOUBLE PRECISION LM
      DIMENSION Y(2)
      COMMON K
      Z=82.0
      LM=1.867825961
      AP=0.729927E-2
      GO TO(1,2),I
    1 G=K*Y(1)/X-((ES-1.0)/LM+Z*AP*V)*Y(2)
      RETURN
    2 G=-K*Y(2)/X+((ES+1.0)/LM+Z*AP*V)*Y(1)
      RETURN
      END
```

REFERENCES

1. Neddermeyer, S.H. and Anderson, C.D., 1937. Phys. Rev. 51, 884.

2. Street, J.C. and Stevenson, E.C., 1937. Phys. Rev. 51, 1005.

3. Anderson, H.L. and Hargrove, C.K., Hincks, E.P., Meandrew, J.D., McKee, R.J., and Barton, R.D., and Kessler, D., 1969. Phys. Rev. 187 , 1565.

4. Fermi, E. and Teller, E., 1947. Phys. Rev. 72, 399.

5. Eisenberg, Y. and Kessler, D., 1961. Nuovo Cimento 19, 1195.

6. Wu, C.S. and Wilets, L., 1969. Ann. Rev. Nucl. Sci. 19, 527.

7. Wheeler, J.A., 1949. Rev. Mod. Phys. 21, 133.

8. Wheeler, J.A., 1953. Phys. Rev. 92, 812.

9. Hofstadter, R., 1957. Ann. Rev. Nucl. Sci. 7, 231.

10. Ford, K.W. and Wills, J.G., 1962. Nuclear Physics 35, 295.

11. Pustovalov, G.E., 1963. Soviet Phys. - JETP 16, 1534.

12. Palit, P., 1964. Physics Letters 11, 82.

13. Cooper, L. and Henley, E., 1953. Phys. Rev. 92, 801.

14. Hill, D.L. and Ford, K.W., 1954. Phys. Rev. 94, 1617.

15. Meyer-Berkhout, U., Ford, K.W. and Green, A.E.S., 1959. Annals of Physics 8, 119.

16. Schiff, L.I., 1968. Quantum Mechanics. (3rd edition) McGraw-Hill Book Co., Inc., New York.

17. Glauber, R. and Rarita, W. and Schwed, P., 1960. Phys. Rev. 120, 609.

18. Foldy, L.L. and Eriksen, E., 1954. Phys. Rev. 95, 1048.

19. Pustovalov, G.E., 1957, Soviet Phys. - JETP 5, 1234.

20. Wichmann, H. and Kroll, N.M., 1956. Phys. Rev. 101, 843.

21. Uehling, E.A., 1935. Phys. Rev. 48, 55.

22. Schwinger, J., 1949. Phys. Rev. 75, 651.

23. Barrett, R.C., Brodsky, S.J., Erickson, G.W. and Goldhaber, M.H., 1968. Phys. Rev. 166, 1589.

24. Backenstoss, G., Charalambus, S., Daniel, H., Koch, H., Poelz, G., Schmitt, H. and Tauscher, L. 1967. Physics Letters 25B, 547.

25. Anderson, H.L., Johnson, C.S. and Hincks, E.P. 1963. Phys. Rev. 130, 2468.

26. Ehrlich, R.D., 1968. Phys. Rev. 173, 1088.

27. Quitmann, D., Engfer, R., Hegel, U., Brix, P., Backenstoss, G., Goebel, K., and Stadler, B., 1964. Nuclear Physics 51, 609.

28. Acker, H.L. and Backenstoss, G., Daum, C., Sens, J.C. and DeWit, S.A., 1966. Nuclear Physics 87, 1.

29. Brix, P., Engfer, R., Hegel, U., Quitmann, D., Backenstoss, G., Goebel, K. and Stadler, B., 1962. Physics Letters 1, 56.

30. Frati, W. and Rainwater, J., 1962. Phys. Rev. 128, 2360.

31. Johnson, C.S., Hincks, E.P. and Anderson, H.L., 1961. Phys. Rev. 121, 283.

32. Backenstoss, G., Geobel, K., Stadler, B., Hegel, U. and Quitmann, D., 1965. Nuclear Physics 62, 449.

33. Bardin, T.T., Barrett, R.C., Cohen, R.C., Devons, S., Hitlin, D., Macagno, E., Nissim-Sabat, C., Rainwater, J., Runge, K. and Wu, C.S., 1966. Phys. Rev. Letters 16, 429.

34. Acker, H.L., Backenstoss, G., Daum, C., Sens, J.C. and DeWit, S.A., 1965. Physics Letters 14, 317.

35. Dieper, W. and Greiner, W., 1968. Nuclear Physics A109, 539.

36. Cole, Jr., R.K., 1969. Phys. Rev. 177, 164.

37. Lakin, W. and Kohn, W., 1954. Phys. Rev. 94, 787.

38. Chen, M.Y., 1968. Ph.D. Thesis, Princeton Univ.

39. Cole, Jr., R.K., 1967. Physics Letters 25B, 178.

40. Skardhamar, H.F., 1970. Nuclear Physics A151, 154.

41. Pustovalov, G.E. and Krechko, M.S., 1960. Nuclear Physics 19, 337.

42. Ford, K.W. and Hughes, V.W. and Wills, J.G., 1963. Phys. Rev. 129, 194.

43. Bethe, H.A., Brown, L.M. and Stehn, J.R., 1950. Phys. Rev. 77, 370.

44. Ralston, A., 1965. A First Course In Numerical Analysis. pp. 191-200, McGraw-Hill Book Co., Inc., New York.

VITA

Surname: KONG Given Names: KAM CHUEN

Place of Birth: CHINA Date of Birth: May 29, 1944

Educational Institutions Attended, with Dates of Entering and Leaving:

THE CHINESE UNIVERSITY OF HONG KONG, HONG KONG 1964 to 1968

Degrees, Diplomas, Etc., Awarded, with Dates and Names of Institutions:

B.Sc. 1968 The Chinese University of Hong Kong.

THE UNIVERSITY OF VICTORIA LIBRARY

MANUSCRIPT DISSERTATION (or THESIS)

AUTHORITY TO DISTRIBUTE

AUTHOR: This dissertation may be lent or microfilm copies made available:

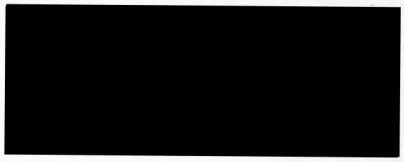

(a) Without restriction

(b) With the restriction that, for a period of five years (until)the written approval of the following is required:

(1) The Chairman, School of Graduate Studies .....

(2) The Author .....

(3) both the Chairman, School of Graduate Studies, and the Author .....

BORROWERS: The borrower undertakes, by signing below, to give proper credit for any use made of the dissertation, and to obtain the consent of the author if it is proposed to make extensive quotations, or to reproduce the dissertation in whole or in part.

Signature of Borrower	Address	Date